tory activity for mesangial cells. We identified gangliosides as a major inhibitory substance in this conditioned medium, suggesting that mesangial cells constitutively shed these substances [21]. Thus, gangliosides are good candidate molecules that regulate mesangial cell responses in glomerular diseases. To date, however, besides a series of indications of the biologic importance of ganglioside shedding, little is known how the shedding of gangliosides is controlled.

In this report, we tested whether biologically distinct forms of cell fate, apoptosis and necrosis, could modulate ganglioside shedding using mesangial cells. The results showed that shedding of gangliosides from mesangial cell membrane markedly increases when these cells die with apoptosis. Such an increase was not apparent when these cells die with necrosis. These results provide the novel link between mesangial cell apoptosis and increased release of gangliosides that potentially suppress mesangial cell proliferation. This is the first evidence indicating that shedding of ganglioside increases when cells are undergoing apoptosis.

METHODS

Cells and transfectant

Rat mesangial cells were grown in culture from isolated glomeruli of an adult male Sprague-Dawley rat. Mesangial cells were identified by their typical elongated and stellar morphology, immunostaining for characteristic cytoskeletal filament protein [α-smooth muscle actin (α-SMA)] [22] and cell-surface antigen (Thy-1) [23]. antibodies used for immunostaining were as follows: mouse antirat Thy-1.1 monoclonal antibody (1:100 dilution; OX-7, Chemicon, Temecula, CA, USA); mouse anti-α–SMA antibody (1:200 dilution; 1A4, Sigma Chemical Company, St. Louis, MO, USA); and goat antimouse immunoglobulin (IgG)-fluorescein isothiocyanate (FITC) (1:80 dilution; Santa Cruz Biotechnology, Santa Cruz, CA, USA). Cells were maintained in 100 mm plate at 37°C with 5% carbon dioxide (CO_2) and fed every 48 hours with Dulbecco's modified Eagle's medium (DMEM)/F-12 (NIKKEN Bio, Kyoto, Japan) supplemented with 10% fetal bovine serum (FBS) (Hyclone, Logan, UT, USA), 100 U/mL penicillin and 100 μg/mL streptomycin (GIBCO BRL, Gaithersburg, MD, USA). The Bcl–XL overexpressing mesangial cell clone was established as follows. The coding lesion of human *Bcl–XL* gene was generated by reverse transcription-polymerase chain reaction (RT-PCR) according to the published sequence [24] and subcloned into the pCR3.1 vector (Invitrogen, Carlsbad, CA, USA). The inserted Bcl–XL fragment was reconstructed in pLXSN retrovirus vector (Clontech, Palo Alto, CA, USA) and pLXSN Bcl–XL that expresses Bcl–XL and neo was created. pLXSN Bcl-XL was transfected into the helper-free ecotropic cell line PT67 (Clontech). Stable transfectants were selected in the presence of the neomycin analog G418 (0.5 mg/mL). Conditioned medium of the G418-resistant cells were used as sources of the Bcl–XL retrovirus. In the presence of 10 μg/mL polybrene, mesangial cells were exposed to retrovirus. Stable infectants were selected in the presence of G418 (0.5mg/mL). As a control, mock-transfected mesangial cells that express neo alone were used.

Induction and evaluation of cell death

Confluent cultures of cells were in serum-free medium exposed to low (10 to 40 mJ/cm^2) and high (400 mJ/cm^2) doses of ultraviolet light to induce apoptosis and necrosis, respectively. Morphologic examination was performed using a phase-contrast microscope. Apoptosis was identified using morphologic criteria, including shrinkage of the cytoplasm, membrane blebbing, and nuclear condensation and/or fragmentation [25]. For fluorescence microscopy, cells were double stained with Hoechst 33258 (10 μg/mL, Sigma Chemical Co.) and propidium iodide (10 μg/mL, Sigma) for 5 minutes. This technique enables quantification of changes in apoptotic rate and exclusion of nonapoptotic cell death, primary necrosis. Viable cells exclude propidium iodide (propidium iodide-negative) and the Hoechst-positive nuclei are round without condensation. When cells undergo apoptosis, the nuclei become condensed and/or fragmented, gradually. These are followed by secondary necrosis (propidium iodide-positive), the final step of apoptosis. When cells die with primary necrosis, cells become propidium iodide-positive without apoptotic features of the nuclei. When a substantial number of cells were detaching, detached cells and attached cells were evaluated separately and total percentages of apoptotic cells were calculated.

Caspase activities were determined by incubation of cell lysate (containing 25 μg total proteins) with 50 μmol/L fluorogenic substrates acetyl-Asp-Glu-Val-Asp-aminomethylcoumarin (Ac-DEVD-AMC; Peptide Institute Inc., Osaka, Japan) in cell-free system buffer, comprising 50 mmol/L N-2-hyydroxyethylpiperazine-N′-2 ethanesulfonic acid (HEPES)-NaOH, pH 7.5, 10% glyceol, and 2 mmol/L dithiothreitol. The release of fluorescent aminomethylcoumarin was measured for 20 minutes by fluorometry (RF-5300PC, Shimadzu, Kyoto, Japan).

Preparation of conditioned medium

To prepare the conditioned medium, confluent mesangial cells grown in 100 mm plates were washed three times with serum-free DMEM/F-12 and incubated in 5 mL serum-free DMEM/F-12 at 37°C. The conditioned medium was collected at each time point specified, then passed through a 0.2 μm filter (Millipore, Bedford, MA, USA), before storage at −80°C until use. The conditioned medium obtained after 8 hours of culture was generally used for cross-feeding experiments.

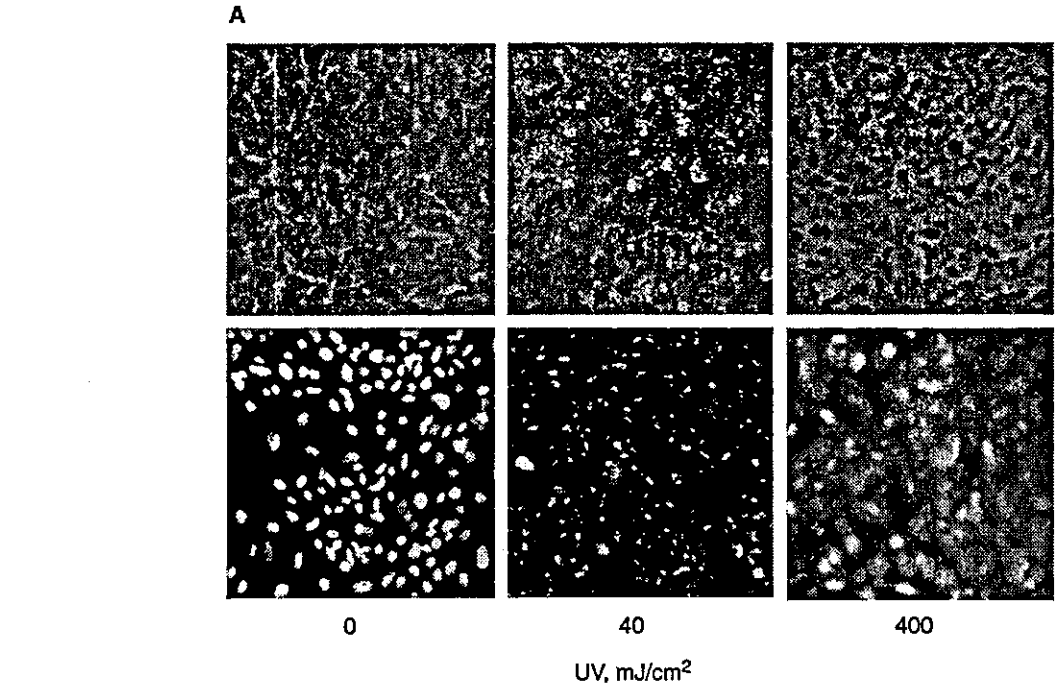

Fig. 1. Induction of cell death in mesangial cells. (*A*) Confluent cultures of mesangial cells were exposed to low (40 mJ/cm²) and high (400 mJ/cm²) doses of ultraviolet (UV) light to induce apoptosis and necrosis, respectively. Morphologic examination was performed using a phase-contrast microscope (upper panel; ×200). Cells were double-stained with Hoechst and propidium iodide for 5 minutes, and analyzed by fluorescence microscopy (lower panel; ×200). (*B*) Membrane vesiculation and blebbing in mesangial cells exposed to low-dose ultraviolet light (40 mJ/cm²).

Cell proliferation assay

A ^{3}H-thymidine incorporation assay was performed to measure the effect of the conditioned medium on DNA synthesis of mesangial cells. Mesangial cells were seeded at a density of 2×10^4 cells/well in a 24-well plate and synchronized in a quiescent state by incubation for 48 hours with fresh medium containing 0.5% FBS. The medium was then replaced with either serum-free medium or conditioned medium from mesangial cells. After 2 hours incubation, the cells were stimulated by adding platelet-derived growth factor (PDGF) (10 ng/mL, Sigma Chemical Co.) and incubated for 20 hours. Subsequently, 2 μCi ^{3}H-thymidine was added to each well for 4 hours. Mesangial cells were washed three times with cold phosphate-buffered saline (PBS) and then incubated in ice-cold 10% trichloroacetic acid for 20 minutes followed

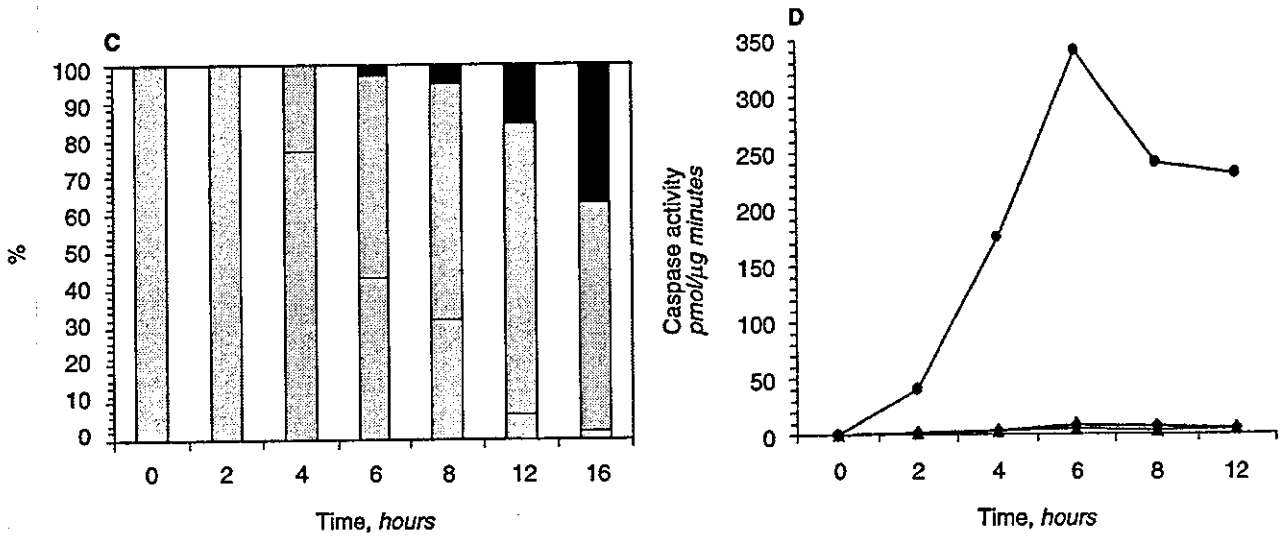

Fig. 1. (Continued) (*C*) Viable cells exclude propidium iodide (PI-negative) and the Hoechst-positive nuclei are round without condensation [blue (B)]. When cells undergo apoptosis, the nuclei become condensed and/or fragmented gradually [blue-condensed (B–C)]. These are followed by secondary necrosis (PI-positive), the final step of apoptosis [red-condensed (R-C)]. (*D*) Caspase activities were determined by incubation of cell lysate (containing 25 μg of total proteins) with 50 μmol/L of the fluorogenic substrate, acetyl-Asp-Glu-Val-Asp-aminomethylcoumarin (Ac-DEVD-AMC), in cell-free system buffer. The release of fluorescent Ac-DEVD-AMC was measured for 20 minutes by fluorometry. Data shown represent one out of three independent experiments with similar results. Symbols are (◆), control; (●), 40 mJ/cm²; (▲), 400 mJ/cm².

by ethyl alcohol for 5 minutes. The cells were solubilized with 0.2 mol/L NaOH and incorporated ^{3}H-thymidine was counted on a liquid scintillation counter. Quadruplicate wells were evaluated for each experiment. Identical cells incubated with 0.5% FBS without replacement of the medium were used as quiescent control.

Biochemical analysis of the conditioned medium

Two milliliters of conditioned medium were placed in micron microconcentrators (Amicon, Inc., Beverly, MA, USA) with molecular mass cutoffs of 3 kD. The microconcentrator was centrifuged at 7500 rpm for 120 minutes at 4°C. The retentate and filtrate were independently collected and the volume was restored to 2 mL. Both preparations were tested for their ability to inhibit mesangial cell growth as described above. The fraction of less than 3 kD was then evaluated for its sensitivity to neuraminidase (type V, 0.1 U/mL at 37°C for 24 hours) (Sigma Chemical Co.).

Metabolic radiolabeling

Rat mesangial cells were seeded at a density of 5×10^6 cells/100 mm plates and cultured for 72 hours. To label the gangliosides, fresh medium was added containing D-[1-^{14}C]-glucosamine HCl and D-[1-^{14}C]-galactose (Amersham Pharmacia Biotech, Amersham, England) to a total of 0.2 μCi/mL culture medium and incubated for 24 hours. The plates were washed five times with PBS and the cells were harvested by trypsinization to be used for the ganglioside purification described below. To obtain gangliosides shed into culture supernatants, radiolabeled cells were further incubated in serum-free medium and the conditioned medium was collected at each time point specified.

Gangliosides purification

Gangliosides were purified according to the method of Ladish and Gillard [26]. Homogenized cell pellets and condition medium were dried by rotary evaporation. A total lipid fraction was obtained by extracting the starting material twice with chloroform/methanol (1:1) with a magnetic string for more than 18 hours at 4°C. For the extraction of radiolabeled gangliosides, 10 μg unlabeled bovine brain gangliosides (Sigma Chemical Co.) was added as cold carrier molecules to optimize the recovery. Gangliosides were isolated by partitioning the dried total lipid extract in diisopropyl ethel, 1-butanol, and 17 mmol/L aqueous NaCl (6:4:5, by volume). Gangliosides in the lower aqueous phase were further purified by Sephadex G-25 gel filtration (Amersham Pharmacia Biotech) to remove salts and other low-molecular-weight contaminants. Overall recovery of gangliosides by this method has been shown to be >90% [26].

Gangliosides analysis

High-performance thin-layer chromatography (HPTLC) analysis of gangliosides was performed, using precoated silica gel 60 HPTLC plates (Merck, Darmstadt, Germany), which were preactivated by heating to 100°C for 60 minutes. The plates were developed in chloroform, methanol, and 0.25% aqueous $CaCl_2 H_2O$ (60:40:9, by volume) to separate gangliosides. Gangliosides were visual-

ized by staining with orcinol spray reagent (Sigma Chemical Co.). Purified bovine gangliosides (Sigma Chemical Co.) were spotted as migration standards. The radiolabeled gangliosides were revealed by exposure of the HPTLC to x-ray film (Eastman Kodak, Rochester, NY, USA) for 14 days at −80°C.

Western blotting

Cells were washed with ice-cold Tris-buffered saline (TBS) buffer (25 mmol/L Tris-HCl, pH 8.0, 120 mmol/L NaCl) and lysed in lysis buffer (50 mmol/L Tris-HCl, pH 8.0, 120 mmol/L NaCl, 0.5% Nonidet P-40, 100 mmol/L sodium fluoride, 200 mmol/L sodium orthovanadate) containing protease inhibitors (10 μg/mL aprotinin, 10 μg/mL phenylmethylsulfonyl fluoride, and 10 μg/mL leupeptin). An equal amount of protein (25 μg) was separated on a 7.5% sodium dodecyl sulfate (SDS)-polyacrylamide gel. Blots were preincubated in TBS buffer containing 5% nonfat dry milk and incubated with 1 μg/mL primary antibodies in TBS buffer containing 5% nonfat dry milk. Following washing, blots were incubated with horseradish peroxidase-conjugated antibodies against mouse or rabbit IgG (1:1000 dilutions; Amersham Pharmacia Biotech, Arlington Heights, IL, USA). For visualization, the enhanced chemiluminescence system (Amersham Pharmacia Biotech) was used according to the manufacturer's protocol. Stripping of membranes was performed at 65°C for 1 hour in 0.2 mol/L glycine, pH 2.5, 0.5 mol/L NaCl, 1% SDS, 0.5% Tween 20. Primary antibodies used in this study were as follows: rabbit anti-Bcl-XL polyclonal antibody (a kind gift from Craig B. Thomson, University of Chicago), and mouse antiactin monoclonal antibody (Clone C4, ICN Pharmaceuticals, Inc., Irvine, CA, USA).

Statistical analysis

Each experiment was performed individually at least three times. The error bars represent the mean SD of one of these experiments and data shown are representative ones of a series of experiments. Comparisons were made with analysis of Student t test. The level of a statistically significant difference was defined as $P < 0.05$.

RESULTS

Induction of cell death in mesangial cells

To test whether distinct forms of cell fate, apoptosis and necrosis, could affect shedding rate of biologically active substance gangliosides, we first evaluated suitable condition for the efficient induction of each type of cell death, apoptosis and necrosis. Confluent cultures of mesangial cells were exposed to low (40 mJ/cm^2) and high doses (400 mJ/cm^2) of ultraviolet light to induce apoptosis and necrosis, respectively. As shown in Figure 1A, viable mesangial cells were propidium iodide-negative and the Hoechst-stained nuclei were round without condensation (Fig. 1A, left panel). When mesangial cells were exposed to low-dose ultraviolet light, more than 96% of mesangial cells died within 16 hours with typical features of apoptosis, including shrinkage of cytoplasm, membrane blebbing, and nuclear condensation (Fig. 1A, middle panel, and B). Figure 1C shows the time course of double-stained mesangial cells (with Hoechst and propidium iodide) exposed to low-dose ultraviolet light. After exposure, the nuclei of mesangial cells started condensation and/or fragmentation by 4 hours. These are followed by secondary necrosis (propidium iodide-positive) around 8 hours after stimulation. In striking contrast, most of the mesangial cells exposed to high-dose ultraviolet light rapidly exhibited positive staining of propidium iodide without apoptotic features, suggesting that these cells died with necrosis (Fig. 1A, right panel).

These results were further confirmed by measuring caspase activation that is specific to apoptosis [27]. As shown in Figure 1D, caspase activity was markedly increased when mesangial cells were exposed to low-dose ultraviolet light, whereas caspase activities remain unchanged in viable unstimulated mesangial cells and those exposed to a high-dose ultraviolet light. These results were consistent with the notion that mesangial cells exposed to low-dose ultraviolet light died with apoptosis, whereas mesangial cells died with necrosis by high-dose ultraviolet light exposure. Supernatants under these conditions were used for the following experiments as conditional medium from viable, apoptotic, or necrotic mesangial cells, respectively.

Enhanced gangliosides shedding by mesangial cells undergoing apoptosis

We next examined whether biologically distinct forms of cellular fate, apoptosis and necrosis, could show effects on ganglioside shedding. As shown in Figure 2, substantial amount of ganglioside-associated radioactivity was seen in the conditioned medium of viable unstimulated mesangial cells. Of note, a nearly twofold increase in the radioactivity was seen in the conditioned medium when mesangial cells were undergoing apoptosis, whereas the increase in the radioactivity was not apparent in conditioned medium from necrotic mesangial cells. These results suggest that shedding of gangliosides by mesangial cells was significantly enhanced when mesangial cells died with apoptosis. A significant amount of ganglioside shedding was observed even at early time points after low doses of ultraviolet light exposure (2 to 4 hours; data not shown), suggesting the importance of these events in the early phase of apoptotic cell death.

Characterization of growth suppressor derived from apoptotic mesangial cells as gangliosides

Recently, we identified that gangliosides are the major growth suppressor in the conditioned medium of mesan-

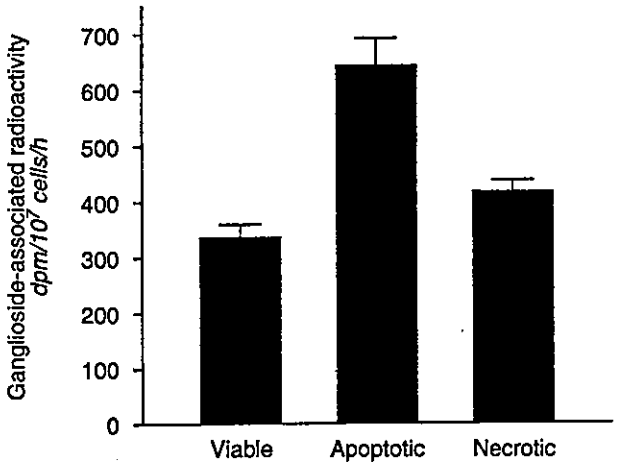

Fig. 2. Enhanced gangliosides shedding by mesangial cells undergoing apoptosis. Mesangial cells were metabolically radiolabeled using labeled sugars and either untreated or treated with low (40 mJ/cm²) and high (400 mJ/cm²) doses of ultraviolet light, respectively. After 8 hours, conditioned medium from each condition of either viable, apoptotic, or necrotic mesangial cells was subjected to the ganglioside purification. Radiolabeled-isolated gangliosides were then quantitatively analyzed by a liquid scintillation counter as ganglioside-associated radioactivity.

gial cells [21]. Conditioned medium of viable, apoptotic, or necrotic mesangial cells were therefore evaluated for growth-regulatory activity in mesangial cells of separate culture. Quiescent mesangial cells were exposed to these conditioned media, followed by PDGF (10 ng/mL) stimulation. To avoid effects of secondary necrosis following the apoptotic process, conditioned media were collected at 8 hours after ultraviolet exposure. As shown in Figure 3A, the DNA synthesis was markedly increased when the cells were cultured in fresh media. When the cells were cultured in conditioned medium of unstimulated viable mesangial cells, however, the increase in DNA synthesis by PDGF was significantly blunted. More strikingly, the PDGF-induced DNA synthesis was almost completely inhibited when mesangial cells were exposed to conditioned medium of apoptotic mesangial cells, whereas the inhibitory effect was not apparent when the cells were exposed to conditioned medium from necrotic mesangial cells.

The inhibitory substance in conditioned medium of apoptotic mesangial cells was next examined for fulfillment of the characteristic criteria of the biologically active monomeric form of gangliosides [28, 29]. The conditioned medium from apoptotic mesangial cells of either more or less than 3 kD were separated by an ultrafiltration membrane and then each fraction was tested for growth inhibitory activity. As shown in Figure 3B, ^{3}[H]-thymidine incorporation assays showed that the growth inhibitory activity obtained from conditioned medium of apoptotic mesangial cells passed through an ultrafiltration membrane with a 3 kD molecular weight cutoff, whereas the fraction that weighed more than 3 kD showed no such effects. In addition, treatment with neuraminidase of the less than 3 kD fraction completely eliminated its inhibitory activity. These results suggest the inhibitory substance derived from apoptotic mesangial cells were less than 3 kD in molecular weight and sensitive to neuraminidase digestion. These characteristics were consistent with those of a monomeric biologically active form of gangliosides [28, 29]. Taken together, these results strongly suggest that increased ganglioside shedding was responsible for the enhanced growth inhibitory activity in conditioned medium from apoptotic mesangial cells.

Suppression of apoptosis and ganglioside shedding by overexpression of antiapoptotic Bcl-XL

We next examined whether the enhanced ganglioside shedding is directly involved in the process of apoptosis. For this purpose, mesangial cells were stably transfected with a plasmid that overexpresses antiapoptotic *Bcl-XL* gene to inhibit apoptosis. In Western blot analysis of the extract from untransfected mesangial cells, the expected 26 kD band was detected (data not shown). In mock transfectant, Bcl-XL proteins were expressed at similar level to those in untransfected cells (Fig. 4A, lane 1). When Bcl-XL was stably overexpressed in mesangial cells, there was an increase in the intensity of the 26 kD band (Fig. 4A, lane 2). Western blot analysis showed complete down-regulation of Bcl-XL proteins in mock transfectant treated with 10 mJ/cm² ultraviolet light (Fig. 4A, lane 3). However, in Bcl-XL transfectants, Bcl-XL protein was still overexpressed, even though the cells were treated with the same doses of ultraviolet light (Fig. 4A, lane 4). As expected, the Bcl-XL transfected mesangial cells were resistant to ultraviolet light–induced apoptosis as compared to that of the mock transfectant (49% in mock transfectant vs. 27% in Bcl-XL transfectant by 10 mJ/cm² ultraviolet light, respectively, Fig. 4 B and C).

Ganglioside shedding was then evaluated in these transfectants, either in unstimulated or ultraviolet–stimulated light. The ganglioside-associated radioactivities were not statistically different between the mock transfectant and Bcl-XL transfectant without ultraviolet light exposure (Fig. 4D). When the mock transfectant was exposed to ultraviolet light (10 mJ/cm²), the ganglioside-associated radioactivity was extremely increased. In contrast, the increase in ganglioside-associated radioactivity by ultraviolet light (10 mJ/cm²) was blunted in the Bcl-XL transfectant as compared to the mock transfectant. These results showed that the increase in gangliosides shedding was significantly attenuated when apoptosis was inhibited by overexpression of antiapoptotic Bcl-XL, even under the same dosage of ultraviolet light exposure. These results strongly suggest that increased rate of ganglioside shedding is directly involved in the process of apoptosis.

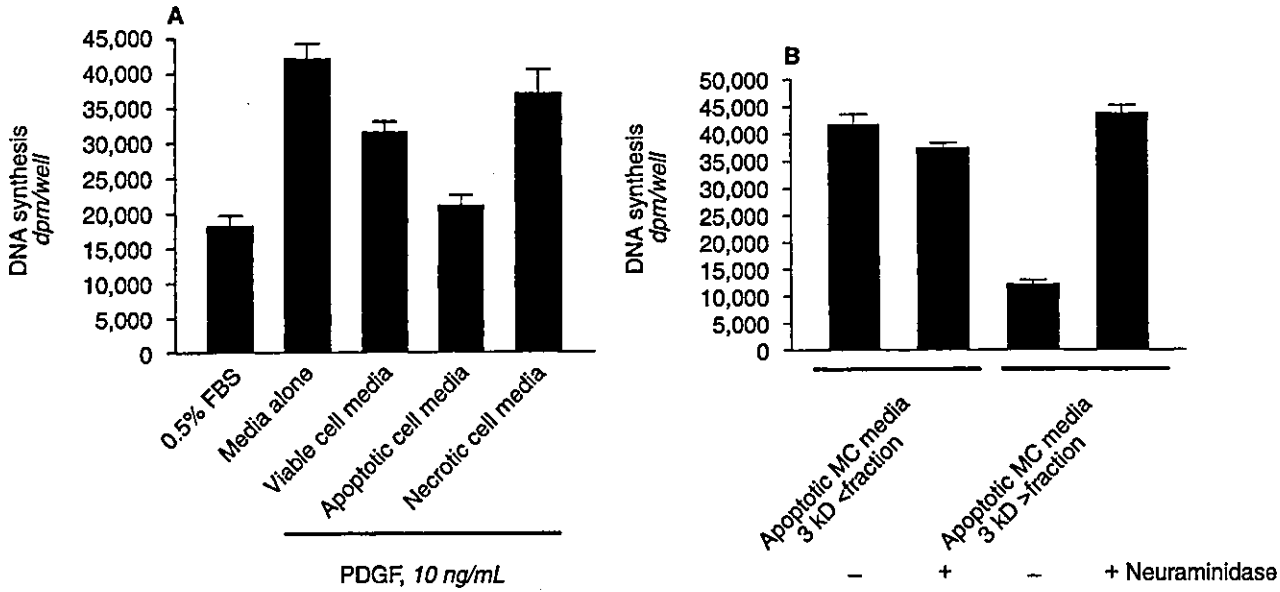

Fig. 3. Characterization of growth suppressor derived from apoptotic mesangial cells as gangliosides. (*A*) The 8 hours of conditioned medium from each condition of either viable, apoptotic, and necrotic mesangial cells were collected. These conditioned media were subjected to growth-inhibitory activity in mesangial cells of separate culture using ^{3}H-thymidine incorporation assay as described in the **Methods** section. The cells incubated with 0.5% fetal bovine serum (FBS) without replacement of the medium were used as quiescent control. PDGF is platelet-derived growth factor. (*B*) The fractions of either more or less than 3 kD in conditioned medium were evaluated for its sensitivity to neuraminidase (0.1 U/mL at 37°C for 24 hours). After treatment, each conditioned medium was subjected to a ^{3}[H]–thymidine incorporation assay, as described in the **Methods** section. MC is mesangial cell.

Enhanced gangliosides shedding in mesangial cells by other inducers of apoptosis

H_2O_2 and staurosporin are known inducers of apoptosis in mesangial cells [30]. We next examined whether the increase in the ganglioside shedding was also observed when these agents other than ultraviolet light were used as inducers of apoptosis. Mesangial cells were metabolically radiolabeled using labeled sugars, washed, and resuspended in fresh media in the presence or absence of H_2O_2 (0.5 μmol/L) and staurosporin (0.1 μmol/L). About 30% to 40% of mesangial cells exposed to these agents exhibited typical features of apoptosis at 16 hours (Fig. 5A). Conditioned media at 8 hours were collected, and subjected to the extraction for gangliosides. Shedding of gangliosides was then analyzed quantitatively by liquid scintillation counting. As shown in Figure 5B, gangliosides–associated radioactivity was significantly increased both by H_2O_2 and staurosporin (27% and 31% increase, respectively) as compared with that of unstimulated control cells. These results suggest that increased shedding of gangliosides in mesangial cells is not specific for ultraviolet light but induced by other inducers of apoptosis.

Comparison of ganglioside composition between viable and apoptotic mesangial cells

We next compared the ganglioside composition between viable and apoptotic mesangial cells, using cell pellets and conditioned medium as starting materials. Gangliosides were extracted from each cell pellet (8 hours after ultraviolet light exposure), and analyzed by HPTLC. As shown in Figure 6A, the HPTLC pattern of cellular gangliosides of apoptotic mesangial cells (and necrotic mesangial cells; data not shown) remained identical to that of viable, untreated cells.

Shed gangliosides into the media were also analyzed for their composition. Mesangial cells were metabolically radiolabeled with labeled sugars, washed and resuspended in fresh medium. After 8 hours, gangliosides were extracted from the conditioned medium and were analyzed by HPTLC autoradiography. Comparison of viable and apoptotic mesangial cell gangliosides are shown in Figure 6B. The HPTLC pattern of shed gangliosides in conditioned medium by apoptotic mesangial cells was almost identical to that of viable cells. Taken together, ganglioside composition was not altered during ultraviolet-induced apoptosis in mesangial cells, either in the cell or in conditioned medium.

DISCUSSION

In the recovery phase of inflammatory diseases, a number of anti-inflammatory molecules are elaborated [31]. Gangliosides were identified from conditioned medium of glomerular mesangial cells as such candidate molecules with an anti-inflammatory potential [21]. However,

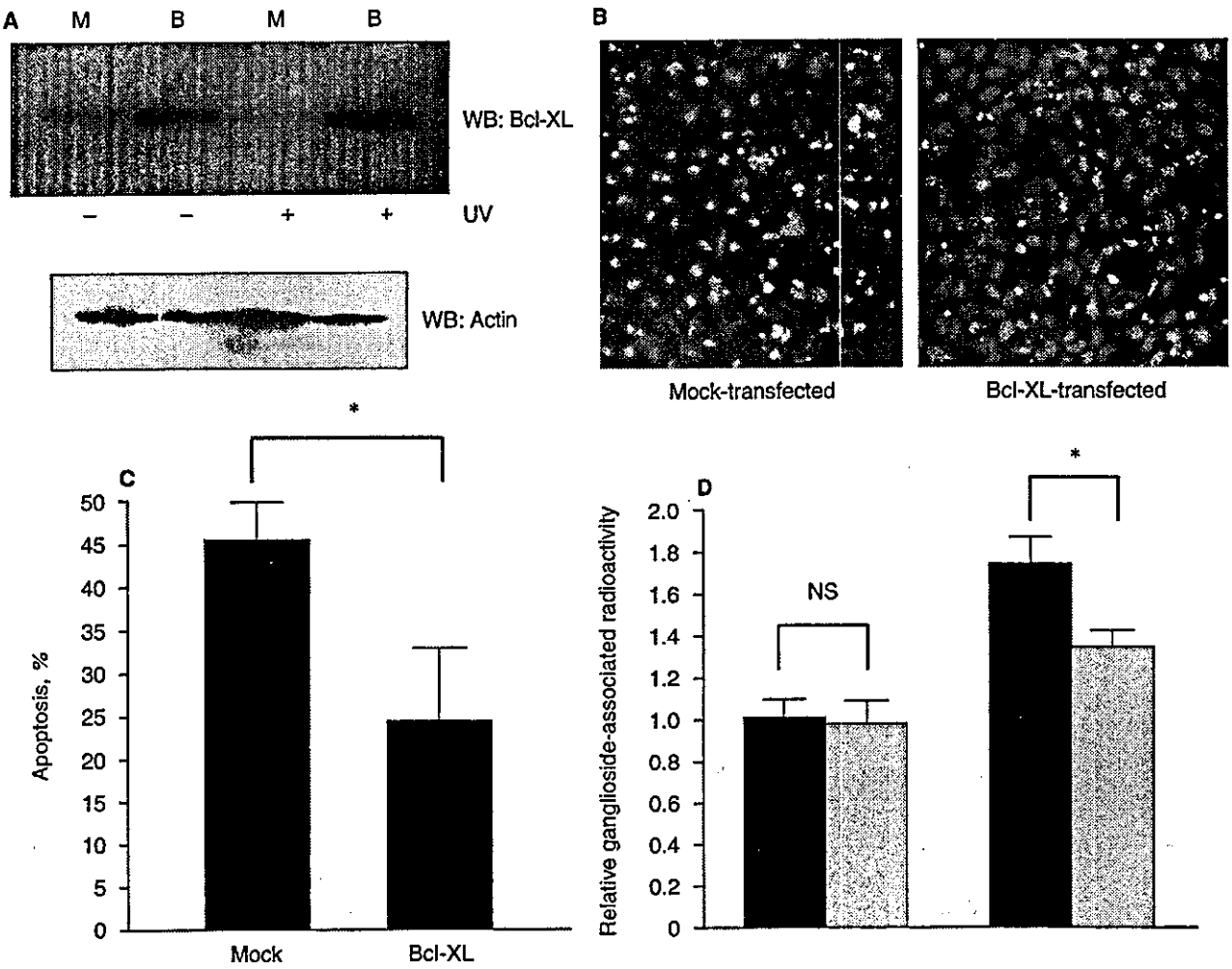

Fig. 4. Suppression of apoptosis and ganglioside shedding by overexpression of antiapoptotic *Bcl-XL* gene. (*A*) Mesangial cells transfected with a control vector (mock) or a vector that expresses Bcl-XL (Bcl-XL) were either untreated or treated with ultraviolet (UV) light (10 mJ/cm^2). After 8 hours of culture, whole cell extracts were prepared and subjected to Western blot analysis using anti-Bcl-XL polyclonal antibody. (*B* and *C*) Twelve hours after ultraviolet light (10 mJ/cm^2) exposure, cells were double-stained with Hoechst and propidium iodide for 5 minutes. The number of viable and apoptotic cells were then counted by fluorescence microscopy in randomly selected three fields/well, and the data were presented as a percentage of cells appearing apoptotic. *$P < 0.05$ vs. mock-transfected. (*D*) Mesangial cells transfected with control vector (mock) (■) or Bcl-XL (Bcl-XL) (▨) were metabolically radiolabeled using lebeled sugars, washed, and resuspended in fresh media, followed by either untreated or treated with ultraviolet light (10 mJ/cm^2). After 8 hours of culture, conditioned media were collected and subjected to the extraction for gangliosides. Radiolabeled isolated gangliosides were then quantitatively analyzed by liquid scintillation counter as ganglioside-associated radioactivity. *$P < 0.05$ vs. mock-transfected.

the metabolism of these molecules, especially the mechanism of shedding, has not been fully explored to date, even in tumor cells by which the ganglioside shedding has been extensively discussed [32, 33]. In this report, we provide evidence that shedding of mesangial cell gangliosides increases when these cells died with apoptosis, a physiologic form of cell death mechanism, which has been extensively observed in many forms of glomerular diseases.

We propose that the shedding of gangliosides from mesangial cells increases when these cells die with apoptosis because of the following reasons. First, the increase was not apparent when these cells died with necrosis, another form of cell death. Second, conditioned medium from apoptotic mesangial cells more substantially inhibited PDGF-induced DNA synthesis in mesangial cells of separate culture, as compared with that from viable or necrotic mesangial cells. In addition, the growth-inhibitory substance in this conditioned medium completely fulfilled characteristic criteria of gangliosides. Third, the increase was significantly suppressed when apoptosis was inhibited by overexpression of antiapoptotic Bcl-XL, even under the same dosage of ultraviolet light exposure. Fourth, increased ganglioside shedding was also relevant

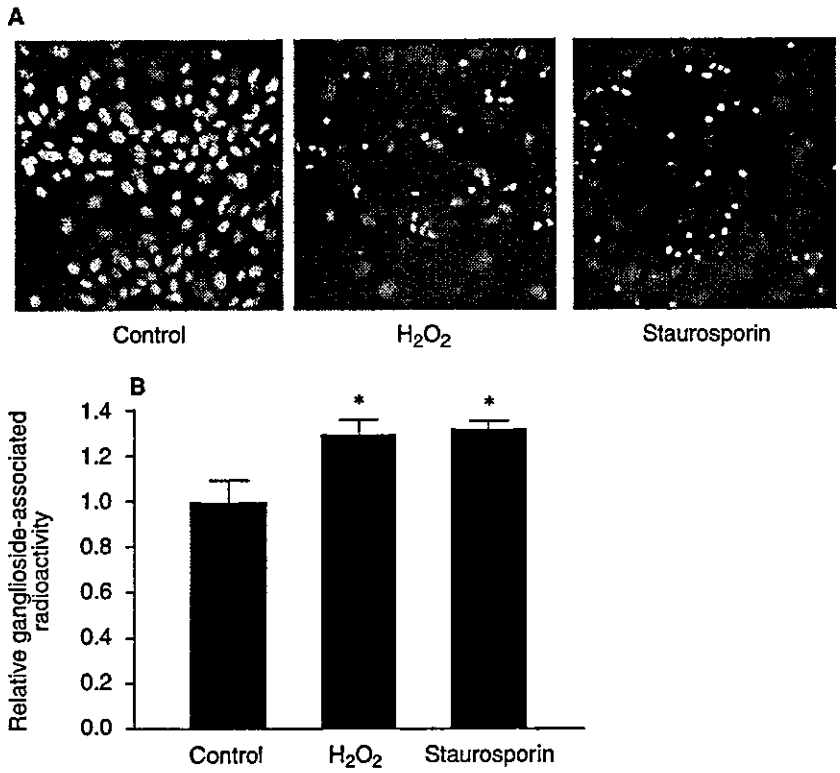

Fig. 5. Enhanced gangliosides shedding in mesangial cells by other inducers of apoptosis. (*A*) Mesangial cells were either untreated or treated with H_2O_2 (0.5 μmol/L) or staurosporin (0.1 μmol/L). After 16 hours, these cells were double-stained with Hoechst and propidium iodide for 5 minutes and were evaluated by fluorescence microscopy. (*B*) Mesangial cells were metabolically radiolabeled using labeled sugars, washed, and resuspended in fresh media in the presence or absence of H_2O_2 (0.5 μmol/L) and staurosporin (0.1 μmol/L). After 8 hours, conditioned media were collected and subjected to the extraction for gangliosides. Radiolabeled isolated gangliosides were then quantitatively analyzed by liquid scintillation counter as ganglioside-associated radioactivity. $^*P < 0.05$ vs. untreated cells (control).

to other proapoptotic stimuli for these cells (H_2O_2 and staurosporin). Finally, composition of shed gangliosides in conditioned medium from apoptotic mesangial cells was almost compatible with that of viable mesangial cells. In addition, we could not detect any differences in ganglioside shedding between cells treated with low doses of ultraviolet light in the presence or absence of *d-threo*-PDMP, a specific inhibitor for ganglioside biosynthesis (data not shown). These observations suggest that altered ganglioside metabolism by cytotoxic stimuli might not contribute to this phenomenon. Furthermore, we found that shedding of gangliosides significantly increased, even in tumor cell lines tested, LAN 5 neuroblastoma and B16 malignant melanoma, when these cells underwent apoptosis by ultraviolet light exposure (data not shown). These results suggest that increased shedding of gangliosides during apoptosis is not specific for mesangial cells.

The mechanisms by which gangliosides are shed from the plasma membrane are not defined at present. Dynamic membrane alterations, such as membrane blebbing and vesiculation, occurred in mesangial cells undergoing apoptosis (Fig. 1B). A recent report by Tapper et al [34] suggested that sphingomyelin hydrolysis to ceramide by sphingomyelinase was crucial for these structural changes at the plasma membrane during apoptosis. In addition, they observed that sphingomyelin breakdown resulted in an increased efflux of cholesterol, which conceivably leads to increased fluidity of the plasma membrane of apoptotic cells. Such membrane destabilization may facilitate shedding of membrane-bound molecules such as gangliosides, as observed in this report. Notably, in our experiments, shedding of gangliosides, as well as the growth-inhibitory effect of conditioned medium, was closely correlated with the induction rate of apoptosis. That was time (0 to 16 hours) and dose of ultraviolet light (2.5 to 40 mJ/cm^2) dependent (data not shown). Ganglioside shedding from mesangial cells was significantly reduced when apoptosis was inhibited by overexpression of the antiapoptotic Bcl-XL (Fig. 4D). In addition, increased shedding of gangliosides was also observed when other inducers of apoptosis were used (Fig. 5). These results suggest that the increase in ganglioside shedding could be induced regardless of each apoptotic signals that are initiated by different stimuli. Rather, the data indicate that the increase in ganglioside shedding during apoptosis may be a passive process following structural alteration at the plasma membrane. The elucidation of the precise natures of these changes in mesangial cell membranes needs further study.

For the efficient and safe resolution of the injured glomerulus, two independent mechanisms, resolution of cell proliferation (by growth suppressors) and resolution of hypercellularity (by apoptosis) must work coordi-

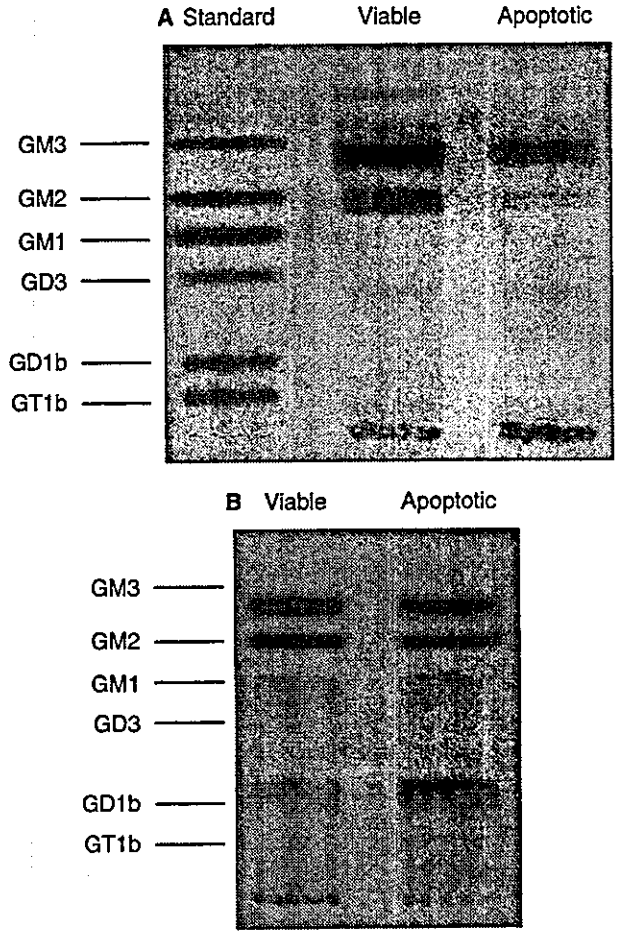

Fig. 6. Comparison of ganglioside composition between viable and apoptotic mesangial cells. *(A)* Mesangial cells either untreated or treated with ultraviolet light (40 mJ/cm^2) were incubated in serum-free media for 8 hours. Gangliosides were extracted from each cell pellet, either viable or apoptotic mesangial cells, and analyzed by high performance thin layer chromatography (HPTLC). The plates were developed in chloroform, methanol, and 0.25% aqueous $CaCl_2$ H_2O (60:40:9, by volume) to separate gangliosides. Gangliosides were then visualized by staining with orcinol spray. Purified bovine gangliosides were spotted as migration standards. *(B)* Mesangial cells were metabolically radiolabeled using labeled sugars, washed, and resuspended in fresh serum-free media, followed by either untreated or treated with ultraviolet light (40 mJ/cm^2) for 8 hours. These conditioned media were then collected and subjected to the extraction for gangliosides. Radiolabeled isolated gangliosides were analyzed by HPTLC autoradiography. After each HPTLC plate was developed, it was exposed to x-ray film for 2 weeks. Each lane contains 2000 dpm ^{14}C-labeled gangliosides.

nately [9, 35]. We observed a close link between apoptosis of mesangial cells and active release of growth-suppressive molecules, gangliosides, by these cells. These results indicate a mechanism for the negative regulation of mesangial cell growth by apoptosis. This may be an ideal mechanism by which actively proliferating mesangial cells are efficiently returned to quiescent state, in the growth factor–rich microenvironment, in parallel with normalization of glomerular cell number. Long-term activation and proliferation of mesangial cells are associated with the altered secretion of extracellular matrices, both quantitatively and qualitatively [36]. Therefore, failure of beneficial clearance of these cells by apoptosis could be a mechanism by which cell populations in the injured glomerulus remain expanded, leading excessive matrix deposition and later scarring. In this respect, evaluating the effects of gangliosides on the metabolism of extracellular matrices will help to understand the pathophysiologic, in vivo, significance of apoptosis in these cells. We are currently investigating these issues.

In summary, our data strongly suggest that shedding of growth-suppressive gangliosides from mesangial cells increases when these cells die with apoptosis. These findings may have an implication for the pathophysiologic significance of mesangial cell apoptosis in glomerular diseases.

ACKNOWLEDGMENTS

This work was supported in part by the grant from the Study Group on IgA Nephropathy and the grant of "Bio–Venture Research Fund Project Aid" from the Ministry of Education, Science and Culture of Japan. We thank Miss Ritsuko Nakayama and Mrs. Shinobu Akita for technical support.

Reprint requests to Nobuo Tsuboi, M.D., Department of Molecular Genetics, Institute of DNA Medicine, Jikei University School of Medicine, 3-25-8 Nishi-Shinbashi, Minato-Ku, Tokyo 105, Japan.
E-mail: nobuotsuboi@aol.com

REFERENCES

1. Wagrowska-Danilewicz M, Danilewicz M: A study of apoptosis in human glomerulonephritis as determined by in situ non-radioactive labeling of DNA strand breaks. *Acta Histochem* 99:257–266, 1997
2. Tashiro K, Kodera S, Takahashi Y, *et al*: Detection of apoptotic cells in glomeruli of patients with IgA nephropathy. *Nephron* 79:21–27, 1998
3. Kodera S, Tashiro K, Ohmuro H, *et al*: A case of lupus nephritis showing good clinical course and apoptosis in glomerular cells detected by the nick end labeling method. *Am J Nephrol* 17:466–470, 1997
4. Bodi I, Abraham AA, Kimmel PL: Apoptosis in human immunodeficiency virus-associated nephropathy. *Am J Kidney Dis* 26:286–291, 1995
5. Baker AJ, Mooney A, Hughes J, *et al*: Mesangial cell apoptosis: The major mechanism for resolution of glomerular hypercellularity in experimental mesangial proliferative nephritis. *J Clin Invest* 94:2105–2113, 1994
6. Shimizu A, Kitamura H, Masuda Y, *et al*: Apoptosis in the repair process of experimental proliferative glomerulonephritis. *Kidney Int* 47:114–121, 1995
7. Sugiyama H, Kashihara N, Makino H, *et al*: Apoptosis in glomerular sclerosis. *Kidney Int* 49:103–111, 1996
8. Ying WZ, Wang PX, Sanders PW: Induction of apoptosis during development of hypertensive nephrosclerosis. *Kidney Int* 58:2007–2017, 2000
9. Savill J: Regulation of glomerular cell number by apoptosis. *Kidney Int* 56:1216–1222, 1999
10. Mooney A, Jobson T, Bacon R, *et al*: Cytokine promote glomerular mesangial cell survival in vitro stimulus-dependent inhibition of apoptosis. *J Immunol* 159:3949–3960, 1997
11. Mooney A, Jackson K, Bacon R, *et al*: Type IV collagen and laminin regulate glomerular mesangial cell susceptibility to apopto-

sis via β_1 integrin-mediated survival signals. *Am J Pathol* 155:599–606, 1999
12. Widmann C, Gibson S, Johnson GL: Caspase-dependent cleavage of signaling proteins during apoptosis: A turn-off mechanism for anti-apoptotic signals. *J Biol Chem* 273:7141–7147, 1998
13. Levkau B, Herren B, Koyama H, *et al*: Caspase-mediated cleavage of focal adhesion kinase pp125FAK and disassembly of focal adhesions in human endothelial cell apoptosis. *J Exp Med* 187:579–586, 1998
14. Meikrantz W, Schlegel R: Suppression of apoptosis by dominant negative mutants of cyclin-dependent protein kinases. *J Biol Chem* 271:10205–10209, 1996
15. Levkau B, Koyama H, Raines EW, *et al*: Cleavage of p21 Cip1/Waf1 and p27Kip1 mediate apoptosis in endothelial cells through activation of cdk2: Role of caspase cascade. *Mol Cell* 1:553–563, 1998
16. Hakomori S: Bifunctional role of glycolipids: Modulators for transmembrane signaling and mediators for cellular interactions. *J Biol Chem* 265:18713–18716, 1990
17. McKallip R, Li R, Ladisch S: Tumor gangliosides inhibit the tumor-specific immune response. *J Immunol* 163:3718–3726, 1999
18. Uzzo RG, Rayman P, Kolenko V, *et al*: Renal cell carcinoma-derived gangliosides suppress nuclear factor-κB activation in T cells. *J Clin Invest* 104:769–776, 1999
19. Ziche M, Morbidelli L, Alessandri G, *et al*: Angiogenesis can be stimulated or repressed in vivo by a change in GM3:GD3 ganglioside ratio. *Lab Invest* 67:711–715, 1992
20. Manfredi MG, Lim S, Claffey KP, *et al*: Gangliosides influence angiogenesis in an experimental mouse brain tumor. *Cancer Res* 59:5392–5397, 1999
21. Tsuboi N, Utsunomiya Y, Kawamura T, *et al*: Gangliosides as an endogenous growth suppressor for glomerular mesangial cells. *Kidney Int* 60(4):1378–1385, 2001
22. Elger M, Drenckhahn D, Nobling R, *et al*: Cultured rat mesangial cells contain smooth muscle alpha–actin not found in vivo. *Am J Pathol* 142:497–509, 1993
23. Otte T, Saito M, Suzuki Y, *et al*: A specific Thy-1 molecular epitope expressed on rat mesangial cells. *Exp Nephrol* 4:350–360, 1996
24. Boise LH, Gonzalez-Garcia M, Postema CE, *et al*: *bcl-x*, a *bcl-2*-related gene that functions as a dominant regulator of apoptotic cell death. *Cell* 74:597–608, 1993
25. Evan G, Littlewood T: A matter of life and cell death. *Science* 281:1317–1322, 1998
26. Ladisch S, Gillard B: A solvent partition method for microscale ganglioside purification. *Anal Biochem* 146:220–231, 1985
27. Thornberry NA, Lazebnik Y: Caspases: Enemies within. *Science* 281:1312–1316, 1998
28. Kong Y, Li R, Ladisch S: Natural forms of shed tumor gangliosides. *Biochim Biophys Acta* 1394:43–56, 1998
29. Olshefski R, Ladisch S: Intercellular transfer of shed tumor cell gangliosides. *FEBS Lett* 386:11–14, 1996
30. Ishikawa Y, Kitamura M: Inhibition of glomerular cell apoptosis by heparin. *Kidney Int* 56:954–963, 1999
31. Kitamura M, Fine LG: The concept of glomerular self-defense. *Kidney Int* 55:1639–1671, 1999
32. Li R, Ladisch S: Abrogation of shedding of immunosuppressive neuroblastoma gangliosides. *Cancer Res* 56:4602–4605, 1996
33. Bernhard H, zum Buschenfelde K-HM, Dippold WG: Gangliosides GD3 shedding by human malignant melanoma cells. *Int J Cancer* 44:155–160, 1989
34. Tapper AD, Ruurs P, Wiedmer T, *et al*: Sphingomyelin hydrolysis to ceramide during the execution phase of apoptosis results from phospholipid scrambling and alters cell-surface morphology. *J Cell Biol* 150:155–164, 2000
35. Johnson RJ: The glomerular response to injury: Progression or resolution? *Kidney Int* 45:1769–1782, 1994
36. Eng E, Floege J, Young BA, *et al*: Does extracellular matrix expansion in glomerular disease require mesangial cell proliferation? *Kidney Int* 45 (Suppl 45): S45-S47, 1994

Kidney International, Vol. 63 (2003), pp. 1302–1312

Specific inhibition of *Egr-1* prevents mesangial cell hypercellularity in experimental nephritis

MARINA CARL, YOSHITAKA AKAGI, SVEN WEIDNER, YOSHITAKA ISAKA, ENYU IMAI, and HARALD D. RUPPRECHT

Med. Klinik IV, University Erlangen-Nürnberg, Erlangen, Germany; Department of Internal Medicine and Therapeutics, Osaka University Graduate School of Medicine, Osaka, Japan; and Med. Klinik Innenstadt, Ludwig-Maximillians University München, München, Germany

Specific inhibition of *Egr-1* prevents mesangial cell hypercellularity in experimental nephritis.

Background. Mesangial cell proliferation is a frequent finding in glomerulonephritis. In cultured mesangial cells, we demonstrated that inhibition of the zinc finger transcription factor, early growth response gene-1 (*Egr-1*), by specific antisense oligonucleotides (AS ODN) blocks mesangial cell proliferation. Therefore, we here investigated the effect of *Egr-1* inhibition on the course of an experimental mesangioproliferative glomerulonephritis in vivo.

Methods. On day 3 after induction of anti-Thy-1.1 nephritis, specific glomerular oligonucleotide transfer was achieved by injection of an oligonucleotide/hemagglutinating virus of Japan/liposome mixture into the left renal artery. The right kidney was left untreated.

Results. Induction of nephritis led to a sixfold induction of *Egr-1* protein on day 6 of disease. This increase in *Egr-1* expression was reduced by 48% in the left kidney by transfer of specific AS ODN. In parallel, the increases in glomerular cellularity, number of mitoses, and glomerular tuft area observed in day 6 nephritic animals were inhibited in the left kidney by 60%, 53%, and 50%, respectively. Changes in the right kidney were not significantly influenced. Likewise, control oligonucleotides showed no effect. Finally, the expression of platelet-derived growth factor-B (PDGF-B), a known target gene of *Egr-1*, was repressed by transfer of specific AS ODN against *Egr-1*.

Conclusion. We conclude that the transcription factor *Egr-1* plays a critical role for mesangial cell proliferation in vivo. Interfering with the induction of *Egr-1* or with its target genes could give rise to novel therapeutic principles in mesangioproliferative glomerulonephritis.

Mesangial cells are specialized pericytes that serve to maintain the delicate architecture of the glomerular capillary tuft and, by means of their contractile properties, also regulate glomerular hemodynamics. Mesangial cells represent approximately 35% to 40% of the total glomerular cell population [1].

One important reaction pattern of mesangial cells to glomerular injury is an increase in proliferation rate and mesangial cell proliferation is a frequent and characteristic finding in many types of glomerular kidney diseases, including membranoproliferative glomerulonephritis (GN), postinfectious GN, immunoglobulin A (IgA) nephropathy, Henoch-Schoenlein purpura, lupus nephritis, or diabetic nephropathy. Mesangial cell proliferation often proceeds and then maintains or accelerates glomerular matrix deposition and sclerosis that ultimately lead to loss of renal function and the need for renal replacement therapy [2]. One potential strategy to prevent progressive renal insufficiency is, therefore, to interfere with early mesangial cell activation and especially mesangial cell proliferation. A factor that we have shown to be intricately linked with mesangial cell proliferation is the transcription factor, early growth response gene-1 (*Egr-1*) [3, 4].

Egr-1, also known as NFGI-A, Krox 24, TIS 8, or zif 268, belongs to the immediate early gene family that also includes the *fos* and *jun* families of transcription factors. It is rapidly and transiently induced after mitogenic stimulation [5, 6], but also after differentiation signals [7, 8], during radiation injury [9], hypoxia [10, 11], depolarization [7], or after induction of apoptosis [12].

The *Egr-1* gene encodes a 75 to 82 kD evolutionarily conserved nuclear phosphoprotein with a DNA binding domain composed of three zinc fingers. *Egr-1* binds specifically to a 5′-GCG(G/T)GGGCG-3′ consensus sequence and acts as a transcriptional activator [13].

We and others have shown that *Egr-1* expression is regulated on the transcriptional level by protein kinase C–dependent and independent mechanisms. Induction involves the interaction between serum response factor (SRF) and ternary complex factor at the serum response element (SRE) consensus sequences in the *Egr-1* pro-

Key words: antisense, transcription factor, mesangioproliferative glomerulonephritis, immediate early gene, liposome.

Received for publication March 26, 2002
and in revised form July 18, 2002
Accepted for publication November 14, 2002

moter [13–15]. The importance of the SREs for *Egr-1* induction was also confirmed in SRF-deficient mice [16].

Several downstream target genes of *Egr-1* have been identified. These include growth factors like the platelet-derived growth factor-A (PDGF-A) [17, 18] or PDGF-B [19], basic fibroblast growth factor (bFGF) [20], transforming growth factor-β (TGF-β) [21], thrombospondin-1 [22], the adhesion molecules CD44 and intercellular adhesion molecule-1 (ICAM-1) [23, 24], the cytokines tumor-necrosis factor-α (TNF-α) and monocyte-colony-stimulating factor (M-CSF), apolipoprotein A1, different cell-cycle components like cyclin D1, p53, Rad, Gαi2, and guanylate cyclase β1 [19, 25, 26], luteinizing hormone (LH)-β [27, 28], and components of the coagulation system like plasminogen activator or tissue factor (TF) [29].

When investigating the functional consequences of *Egr-1* deficiency, Lee et al [27, 28] noted that, in embryonic stem cells with an inactivated *Egr-1* gene, growth and differentiation proceed normally. Similarly, *Egr-1*–deficient mice develop normally without an apparent phenotype except for female infertility. Female mice are infertile because of LH-β deficiency and infertility is successfully reversed by LH-β substitution. The LH-β promotor was shown to bear an *Egr-1* consensus sequence and to be responsive to *Egr-1* [27, 28].

Under some specific disease situations, a pathologic phenotype of *Egr-1*–deficient mice becomes apparent. In a murine model of normobaric hypoxia, pulmonary fibrin deposition is a result of a rapid expression of *Egr-1*, which consecutively leads to transcription and expression of TF in the hypoxic lung. In contrast *Egr-1*–deficient mice subjected to hypoxia displayed neither TF expression nor was intravascular fibrin deposition detectable [11]. Furthermore, *Egr-1* is overexpressed in a majority of prostate cancers [30–32] and is implicated in the regulation of several genes important for prostate tumor progression. In *Egr-1* knockout mice it was demonstrated that *Egr-1* deficiency did not prevent tumor initiation or tumor growth rate; however, *Egr-1* deficiency significantly delayed the transition from localized carcinoma in situ to invasive carcinoma [33].

In addition to these experiments in *Egr-1*–deficient mice, several potentially important functions of the transcription factor *Egr-1* have been characterized in various disease models. While *Egr-1* is expressed at low or undetectable levels in the normal rat artery wall, it is dramatically induced following mechanical injury [34, 35]. Smooth muscle cell (SMC) proliferation is a key event in blood vessel repair after arterial injury and Santiago et al [36, 37] were able to show that SMC proliferation and regrowth after scraping injury in vitro were both inhibited by antisense oligonucleotides (AS ODN) against *Egr-1*. More important, the same authors demonstrated using DNA enzyme technology to inhibit *Egr-1* induction that SMC proliferation could not only be prevented in vitro but also in vivo in a balloon injury model of the rat carotid artery wall, where excessive neointima formation was prevented [38]. High-level expression of *Egr-1* and *Egr-1*–induced genes was also found in mouse and human atherosclerotic lesions, predominantly in SMC and endothelial cells [39].

Our studies in cultured mesangial cells demonstrated that *Egr-1* induction closely correlated with mesangial cell proliferation. Specific AS ODN directed against *Egr-1* inhibited *Egr-1* expression on the mRNA and protein level and dose-dependently prevented PDGF, endothelin-1 or serum-induced mesangial cell proliferation in vitro [3, 4]. Several AS ODN were tested and their ability to block *Egr-1* induction closely correlated with their potential to block mesangial cell proliferation. Control ODN were without detectable effects. Furthermore, we found that nitric oxide application induced inhibition of mesangial cell proliferation by interfering with binding of *Egr-1* to its DNA recognition sequence [40]. In the anti-Thy-1.1 nephritis, an experimental mesangioproliferative GN model in the rat, glomerular *Egr-1* expression increased sixfold on day 6 of nephritis, which coincides with the maximal mesangioproliferative activity observed in this model in vivo.

In the current study we, therefore, wanted to investigate whether inhibition of *Egr-1* expression in vivo in a rat model of mesangioproliferative GN interfered with mesangial cell mitogenesis. For this purpose, specific AS ODN against *Egr-1* were delivered to the mesangial compartment using the hemagglutinating virus of Japan (HVJ)/liposome method. This method was successfully used before for specific gene transfer to the glomerulus and especially to mesangial cells [41–44].

METHODS

Experimental disease

In 4-week-old male Sprague-Dawley rats (150 g; Charles River, Sulzfeld, Germany) experimental GN was induced by injection of monoclonal antibody (mAb) ER4, directed against the Thy-1.1 antigen (1 mg/kg body weight; Antibody Solutions, Palo Alto, CA, USA) into the tail vein [45]. On day 3 of disease, different ODN were transferred using the HVJ/liposome method. On day 4, 6, or 10 of disease, rats were perfused with 100 mL phosphate-buffered saline (PBS) via the abdominal aorta, renal tissue was prepared for histochemistry, and glomeruli were isolated by a sequential sieving technique (mesh size, 180 μm, 125 μm, or 75 μm) [5] for preparation of glomerular protein.

ODN used for the study

Sequences of phosphothioate-modified antisense (AS), scrambled (SCR), and mismatched (M) ODN (MWG,

Biotech, Ebersberg, Germany) and their positions relative to the translational AUG start site:

AS1: 5'-GCGGGGTGCAGGGGCACACT-3' (−118 to −99)

SCR1: 5'-AGGCTGGCTGCCGGGAGCGA-3'

AS2: 5'-TTACATGCGGGGTGC-3' (−107 to −93)

AS2M4: 5'-TCAGATGTGGGGTCC-3'

Twenty-five percent of ODNs were labeled with fluorescein at the 5'-end for visualization of a successful transfer of ODN in kidney biopsy probes.

HVJ/liposome method for the in vivo transfer of ODN

Culture of HVJ. Chorioallantoic membranes of chicken eggs with 10-day-old embryos were vaccinated with 100 μL virus concentrate (1:1000 in polypeptone). Vaccinated eggs were incubated at 36°C for 3 days. The chorioallantoic fluid containing the virus was harvested and centrifuged (1000*g*, 4°C, 10 minutes). To isolate the virus, the supernatant was centrifuged (27,000*g*, 4°C, 30 minutes), the pellet was resolved in balanced salt solution (BSS) (140 mmol/L NaCl, 5.4 mmol/L KCl, 10 mmol/L Tris HCl, pH 7.6) and incubated overnight at 4°C. This isolation step was repeated, the pellet was suspended in BSS, low-speed centrifuged to remove aggregated virus particles and resuspended in BSS [46].

Preparation of lipid mixture. Phosphatidylserine (Sigma-Aldrich, Taufkirchen, Germany), phospatidylcholine (Avanti Polar Lipids, Inc., Alabaster, AL, USA), and cholesterol (Sigma-Aldrich) were mixed at a weight ratio of 1:4.8:2 in chloroform. The lipid mixture (10 mg) was dried on the wall of a specific glass tube (Ø2 cm, Rettberg GmbH, Götttingen, Germany), with the tip of the tube immersed in a 45°C water bath in a rotary evaporator to obtain a uniformly thin lipid layer.

Preparation of ODN-containing liposomes. ODN (200 μg) in 200 μL BSS were added to the dried lipids into the glass tube. Unilamellar liposomes containing ODN were obtained by 8 vortexing-incubation cycles (vortexing 30 seconds, incubating 30 seconds at 37°C) and by a final sonication step for 4 seconds in a water bath sonicator (Sonorex; Bandelin Electronics, Berlin, Germany). After adding 300 μL BSS, the glass tube was incubated in a shaking water bath (120 rpm, 30 minutes, 37°C). To obtain ODN containing HVJ/liposomes, ultraviolet-inactivated (100 erg/mm²/second) virus particles were added to ODN liposome mixture and incubated in a shaking water bath (120 rpm, 1 hour, 37°C). ODN containing HVJ/liposomes were isolated by sucrose gradient ultracentrifugation (24,000 rpm, 3 hours, 4°C). The ODN/HVJ/liposomes complexes were observed as broad band in a layer between BSS and the 30% sucrose solution. The ODN/HVJ/liposomes complexes were stored for a maximum of 24 hours at 4°C before transfer to the kidney. The content of one glass tube was used per animal.

Injection of ODN/HVJ/liposome complexes. Nephritic rats were anesthetized by intraperitoneal injection of pentobarbital (50 mg/kg body weight). A catheter (Insyte-W 24GA/0.75IN, Becton Dickinson, Heidelberg, Germany) was inserted into the left renal artery via the abdominal aorta, and the suprarenal aorta was clipped with a vessel clamp (Micro Serrefines 18055-01, Fine Science Tools, Heidelberg, Germany). $CaCl_2$ (final concentration, 1 mmol/L) was added to the ODN containing HVJ/liposome solution and 500 μL of the solution were then injected into the left renal artery and incubated for 10 minutes under ischemic conditions. After the incubation period, the catheter was removed and the punction site was closed with Superglue and the kidney was reperfused. The solution was only transferred into the left kidney, the right kidney was left untreated.

Kidney biopsies were taken 10 minutes after the kidney was reperfused and the tissue was shock frozen in liquid nitrogen. Animals, in which only the Thy-1.1 nephritis was induced by antibody injection and no ODN transfer was performed ("no oligo" control rats), and also control animals (control) without any treatment were not subjected to aortic clamp or renal perfusion with carrier and renal ischemia.

Immunohistochemistry. To control for successful transfer of ODN, 3 μm cryostat frozen sections of the renal biopsy specimen were air dried (10 minutes), fixed in acetone (10 minutes, −20°C), washed in PBS, and mounted with Moviol (Merck, Darmstadt, Germany). Fluorescein isothiocyanate (FITC)-labeled ODN were visualized by fluorescence microscopy (Leica DMR, Filter L4 BP 450-490; Leica Microsystems GmbH, Wezlar, Germany).

To costain for mesangial cells, frozen sections were additionally incubated with mAb anti-Thy-1.1 OX7 (1:100 in PBS) (Serotec, Oxford, UK) for 1 hour, reverse transcription (RS), washed with PBS, and incubated with a secondary Cy3-labeled antimouse IgG Ab (1:200 in PBS; Serotec). FITC-labeled ODN and OX7 staining were visualized by fluorescence microscopy (Leica DMR, Filter G/R 490/20//575/30).

Determination of glomerular cell number, tuft area, and number of mitotic figures. For evaluating glomerular cell number, tuft area, and number of mitotic figures paraformaldehyde (5%) fixed, paraffin-embedded tissue sections (2 μm, 4 μm) were treated with 100% xylol, rehydrated in 100%, 95%, and 70% ethanol. After washing in PBS, the sections were stained with hematoxylin (3 seconds), washed in water (10 minutes), then stained with eosin (2 seconds), and washed (5 minutes). After dehydrating in 95%, 100% ethanol, and 100% xylol, the sections were mounted with Entellan (Merck). Glomerular tuft area was determined using Leica DMR microscope (×400) with Hyperion image analysis software (Dietermann und Heuser Solution GmBH, Greifenstein-Beilstein, Germany). Mitotic figures were counted in 548 to 1261 glomeruli of three to five experimental animals and numbers are given as mitotic figures per 100 glomeruli.

Protein extraction, Western blot analysis. Isolated glomeruli from rat kidneys were lysed by repeated freeze/thaw cycles in radioimmunoprecipitation assay (RIPA) solution [50 mmol/L Tris HCl, pH 7.2; 10 mmol/L ethylenediaminetetraacetic acid (EDTA), pH 7.2; 150 mmol/L NaCl; 0.1% sodium dodecyl sulfate (SDS); 1% sodium decholate; 1% Triton X-100; 1 mmol/L phenylmethylsulfonyl fluoride (PMSF); 2 μg/mL leupeptin; and 100 μmol/L sodium orthovanadate]. After Ultra turrax sonication (2 × 30 seconds, 24,000 rpm) (Ultra turrax T25; Janke und Kunkel Labortechnik, Staufen, Germany), the suspension was centrifuged (10,000 rpm, 10 minutes, 4°C) and protein concentration was determined using the Pierce Protein assay (Pierce, Rockford, IL, USA) according to manufacturer's instructions.

Protein samples containing 30 μg total glomerular protein were denatured by boiling (5 minutes) and separated on a 7.5% SDS-polyacrylamide gel (SDS-PAGE) under reducing conditions. The gels were electroblotted onto nitrocellulose (NC) membranes (Amersham Pharmacia Biotech Europe GmbH, Freiburg, Germany), and the transfer was controlled by Ponceau-S staining. Membranes were blocked in PBS containing 0.5% Tween 20 and 5% nonfat dry milk powder to inhibit unspecific binding (1 hour, RT). The membranes were incubated with the primary anti-*Egr-1* Ab (1:1000 in PBS/Tween; *Egr-1* C19, Santa Cruz Biotechnology, Santa Cruz, CA, USA; 1 hour, RT). *Egr-1* was visualized with a secondary horseradish peroxidase–conjugated antirabbit IgG Ab (1:15000 in PBS/Tween; Pierce) using ECL Pierce Super Signal Kit system (Pierce). *Egr-1* expression was quantified by scanning densitometry. To stain for PDGF-B blots were incubated with anti-PDGF-B Ab (1:1000 in PBS/Tween; PDGF-B H55, Santa Cruz Biotechnology; 1 hour, RT).

Statistical analysis

Statistical analysis was performed using Student *t* test for unpaired samples.

RESULTS

HVJ/liposome method mediates specific transfer of ODN into glomerular mesangial cells

On day 3 after induction of anti-Thy-1.1 nephritis, FITC-labeled AS ODN against *Egr-1* incorporated into HVJ/liposomes were injected into the left renal artery and incubated for 10 minutes under ischemic conditions. After 10 minutes of reperfusion, a kidney biopsy was taken and snap-frozen in liquid nitrogen. Only those animals were used for further investigation, in which cryostat sections revealed a successful transfer of FITC-labeled AS ODN to nearly all glomeruli of the left injected kidney (Fig. 1A). Transfer was observed mainly to nuclei of cells in mesangial position (Fig. 1B). By costaining with the mAb OX7, a specific mesangial cell surface marker, we could demonstrate that the ODN were indeed delivered predominantly into mesangial cells (Fig. 1C). A detectable glomerular ODN transfer into the right uninjected kidney did not occur (Fig. 1D).

Specific AS ODN against *Egr-1* inhibits glomerular *Egr-1* expression during experimental anti-Thy-1.1 nephritis

A total of 200 μg of specific AS ODN against *Egr-1* (AS2) or mutated control ODN (AS2M4) were injected into the left kidney 3 days after induction of anti-Thy-1.1 nephritis using the HVJ/liposome method. On day 6 of nephritis, glomerular protein lysates were prepared and tested for expression of *Egr-1* protein by Western blot analysis (a representative of three experiments is shown in Fig. 2). We selected day 6 of the disease for our tests because mesangial cell proliferation as well as *Egr-1* expression are maximal on this day, as demonstrated in our earlier studies [4]. Compared to control animals, nephritic rats showed a sixfold increase in *Egr-1* protein expression. This expression was significantly reduced by 48 ± 3% only in the left kidney of AS2 ODN transferred rats, whereas the glomerular *Egr-1* expression in the right uninjected kidney of AS2 ODN transferred rats was only minimally reduced (−13 ± 1%). After transfer of mutated control ODN (AS2M4), *Egr-1* expression remained nearly unaffected, both in the injected left as well as in the uninjected right kidney.

Similar results were obtained when a different AS ODN (AS1) was used and *Egr-1* expression was analyzed by immunoprecipitation and Western blot (data not shown). We were, therefore, able to specifically inhibit glomerular *Egr-1* protein induction in the left kidney of nephritic animals by using an HVJ/liposome–mediated transfer of AS ODN against *Egr-1*.

Specific AS ODN against *Egr-1* prevents glomerular hypercellularity and tuft enlargement in anti-Thy-1.1 nephritis

In Figure 3, the histologic changes induced by anti-Thy-1.1 nephritis and their partial reversion by injection of AS ODN against *Egr-1* into the left kidney are shown. As compared to control kidney (Fig. 3A), a massive extension in glomerular tuft area, as well as an increase in glomerular cell number, is seen on day 6 of anti-Thy-1.1 nephritis (Fig. 3B). These morphologic alterations were partially reversed only in the left injected kidney (Fig. 3C) of specific AS ODN–transferred rats, but not in the right uninjected kidney (Fig. 3D). Transfer of control ODN had no visible effect on glomerular histology (data not shown).

To further validate these observations, the number of nuclei per glomerular cross-section was counted in 50 glomeruli of control rats ($N = 3$), of day 6 nephritic rats

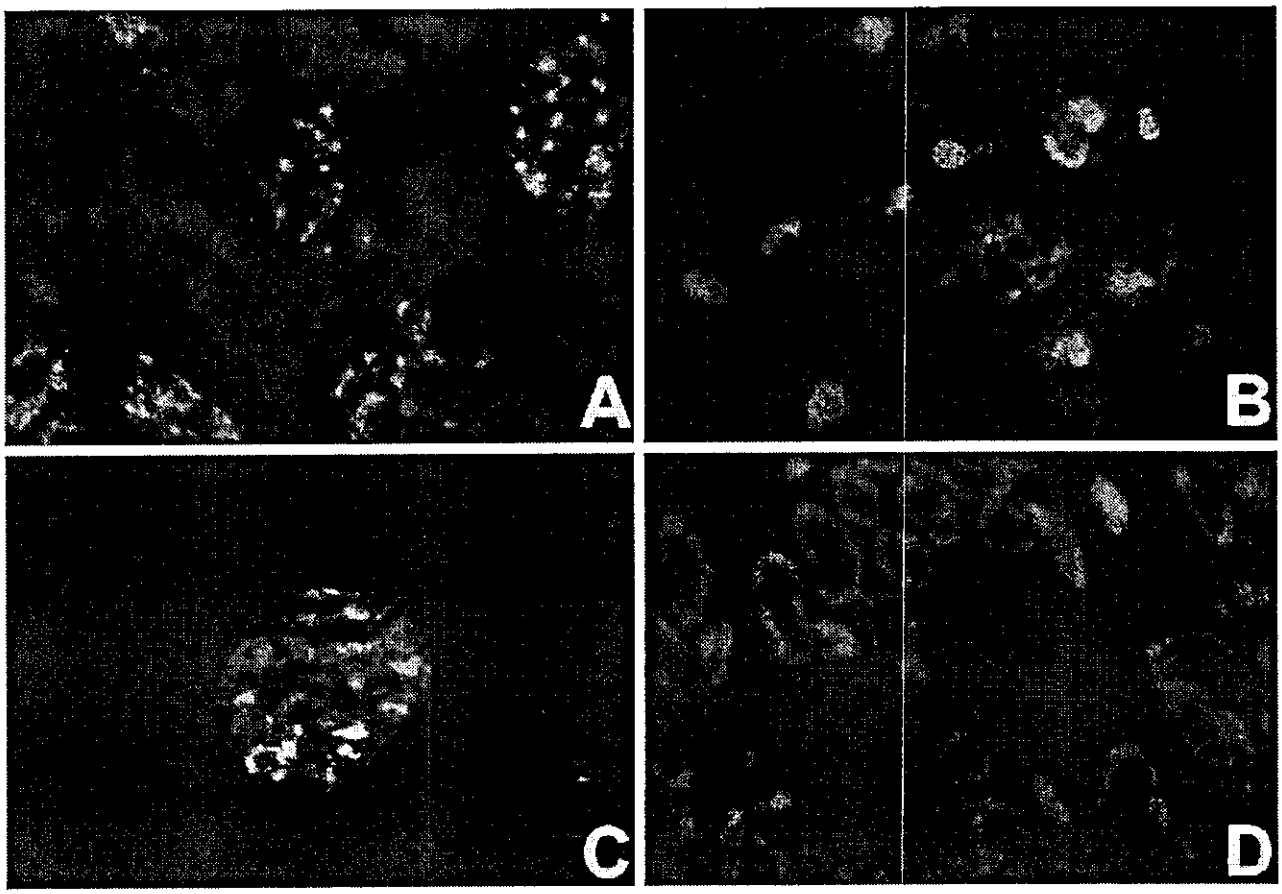

Fig. 1. Hemagglutinating virus of Japan (HVJ)/liposome-method mediates targeted transfer of fluorescein isothiocyanate (FITC)-labeled oligonucleotides (ODN) into glomerular mesangial cells of the left kidney. Three days after induction of anti-Thy-1.1 nephritis, FITC-labeled antisense (AS) ODN against *Egr-1* incorporated into HVJ/liposomes were injected into the left renal artery and incubated for 10 minutes under ischemic conditions before reperfusion of the kidney was allowed. After 10 minutes of reperfusion, a kidney biopsy was taken from the lower pole and snap-frozen in liquid nitrogen. Successful transfer of ODN was visualized by fluorescence microscopy of 3 μm cryostat sections. *(A)* and *(B)* Transfer of FITC-labeled ODN into glomeruli of the left kidney (×400; ×1000). *(C)* Costaining with anti-Thy-1.1 antibody (Ab) OX7 demonstrates specific transfer to nuclei of glomerular mesangial cells (×400). *(D)* No specific staining is observed in the right uninjected kidney (×400).

($N = 3$), in the left and right kidney each of AS1 ($N = 5$) or AS2 ($N = 3$) ODN–injected nephritic rats and in the left and right kidney each of SCR1 ($N = 4$) or AS2M4 ($N = 4$) control ODN–injected nephritic animals.

The increase in glomerular cell number on day 6 of nephritis was significantly inhibited in the left kidney by transfer of specific AS ODN (AS1, AS2) against *Egr-1* by 54% and 65%, respectively (Fig. 4).

Neither transfer of scrambled (SCR1) nor mutated (AS2M4) control ODN influenced glomerular cell number. A slight, albeit not significant, suppression of the increase in glomerular cell number was observed in the right uninjected kidney of AS ODN–transferred rats. This is in accordance with the consistently observed slight reduction in glomerular *Egr-1* protein expression in the right kidney of AS ODN–injected nephritic animals (see Fig. 2). The antiproliferative effect of AS ODN against *Egr-1* was still observed on day 10 of nephritis, where a 39% reduction of the increase in cell number per glomerular cross-section was noted (data not shown). Comparable results were obtained when we measured the glomerular tuft area (Fig. 5). The increase in glomerular tuft area seen in day 6 nephritic animals was significantly diminished by about 50% only in the left kidney of AS ODN (AS1/AS2)–transferred rats. Tuft area enlargement in the right uninjected kidney of AS ODN–transferred rats or in control ODN-treated rats was not significantly altered.

Specific transfer of AS ODN against *Egr-1* reduces the number of mitotic figures in anti-Thy-1.1 nephritis

To further substantiate our data, the number of glomerular mitotic figures was counted in healthy control animals, in nephritic animals, and in ODN-injected animals (Fig. 6). The number of mitotic figures per 100 glomeruli increased from 2/100 in control animals to 13/

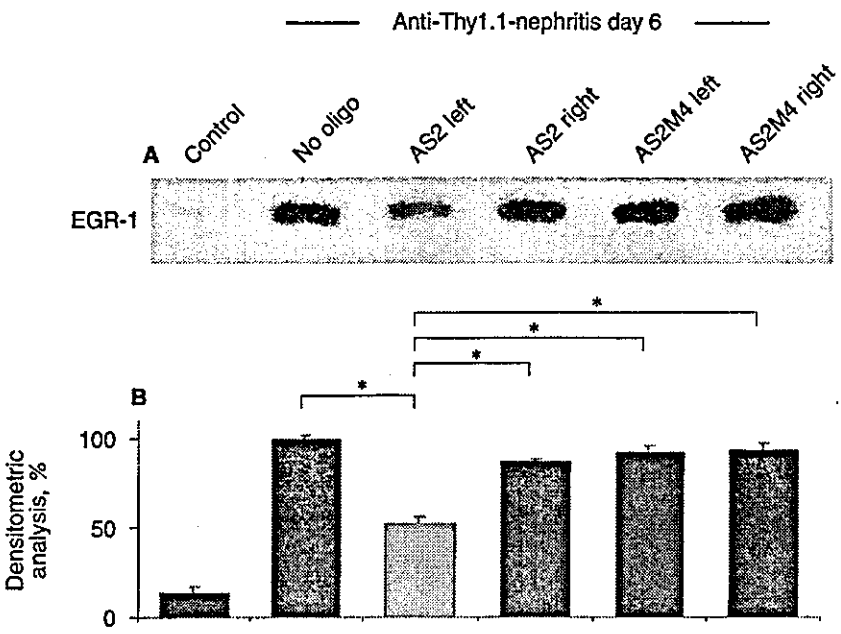

Fig. 2. Inhibition of glomerular *Egr-1* expression by specific antisense oligonucleotides (AS ODN) against *Egr-1* during experimental anti-Thy-1.1 nephritis. Three days after induction of mesangioproliferative anti-Thy-1.1 nephritis, AS ODN against *Egr-1* (AS2) or mutated control ODN (AS2M4) were transferred into the left kidney by the hemagglutinating virus of Japan (HVJ)/liposome method. On day 6 of nephritis, animals were sacrificed, kidneys were removed, and glomeruli were isolated by the differential sieving technique. Glomerular protein lysate (30 μg) was separated by sodium docedyl sulfate-polyacrylamide gel phoresis (SDS-PAGE) and blotted onto NC membranes. *Egr-1* protein was detected by a polyclonal *Egr-1* antibody (Ab) and a secondary horseradish peroxidase-conjugated antirabbit immunoglobulin (IgG) Ab using the Pierce Super Signal Detection system. Specific inhibition of glomerular *Egr-1* protein expression is only observed in the left kidney (AS2 left) of AS ODN-injected animals, not in the right kidney (AS2 right) or in the kidneys of control ODN-injected animals (AS2M4 left; AS2M4 right). *(A)* Western Blot analysis showing a representative of three independent experiments. *(B)* Densitometric analysis of three independent experiments. Glomerular *Egr-1* protein expression in Thy-Thy-1.1 animals not treated with ODN is set at 100%; average ± SD of three experiments is shown. $*P < 0.05$

100 on day 4 and to 17/100 on day 6 of anti-Thy-1.1 nephritis. Both on day 4 and on day 6 of anti-Thy-1.1 nephritis, transfer of specific AS ODN against *Egr-1* (AS2) considerably inhibited the number of mitotic figures in the left kidney (−46% on day 4, −53% on day 6). Again, no significant changes were seen in the right kidney of AS ODN–injected animals or in the kidneys of control ODN (AS2M4)–injected animals.

As already shown in our previous studies, AS ODN against *Egr-1* also inhibits proliferation of cultured rat mesangial cells [3]. Quiescent mesangial cells were incubated with specific AS ODN for 16 hours before stimulating with 4% fetal calf serum (FCS). AS ODN with pronounced effects on *Egr-1* protein expression (AS1, −55%; AS2, −47%) proved to be potent inhibitors of mesangial cell growth (AS1, −46%; AS2, −38%). In contrast, an AS ODN against *Egr-1* (AS3) that was ineffective in blocking *Egr-1* induction failed to suppress mesangial cell growth and mutated, and scrambled control ODN had no effect on mesangial cell proliferation in culture [3] (data not shown).

Glomerular transfer of specific AS ODN against *Egr-1* inhibits glomerular expression of the *Egr-1* target PDGF-B

In its function as a transcriptional activator *Egr-1* regulates the induction of specific target genes. One of the *Egr-1* target genes also linked to mesangial cell proliferation is PDGF-B. PDGF-B expression increased approximately 16-fold from control animals to day 6 nephritic animals. We, therefore, investigated the glomerular expression of PDGF-B, after transfer of AS ODN against *Egr-1* (Fig. 7). Corresponding to the inhibition of *Egr-1* expression, seen in Figure 2, transfer of AS ODN against *Egr-1* (AS2) by the HVJ/liposome method repressed the glomerular PDGF-B protein expression in the left kidney by 55%, whereas the glomerular PDGF-B expression in the right uninjected kidney of AS2 injected rats and in mutated control ODN (AS2M4)–injected rats was not influenced.

DISCUSSION

Glomerular hypercellularity is one of the histopathologic hallmarks of GN and can lead, if not successfully reversed by repair processes, to progressive glomerular extracellular matrix deposition and sclerosis and ultimately to loss of renal function and end-stage renal disease.

In our previous work, we could demonstrate a strong up-regulation of the transcription factor *Egr-1* in an in vivo model of mesangioproliferative GN, the anti-Thy-1.1 model in the rat. Our studies also revealed a direct correlation between *Egr-1* up-regulation and mesangial cell proliferation, since maximal *Egr-1* expression that was observed on day 6 of the disease coincided with the strongest proliferative activity in this model. The role of *Egr-1* for mesangial cell proliferation was further sub-

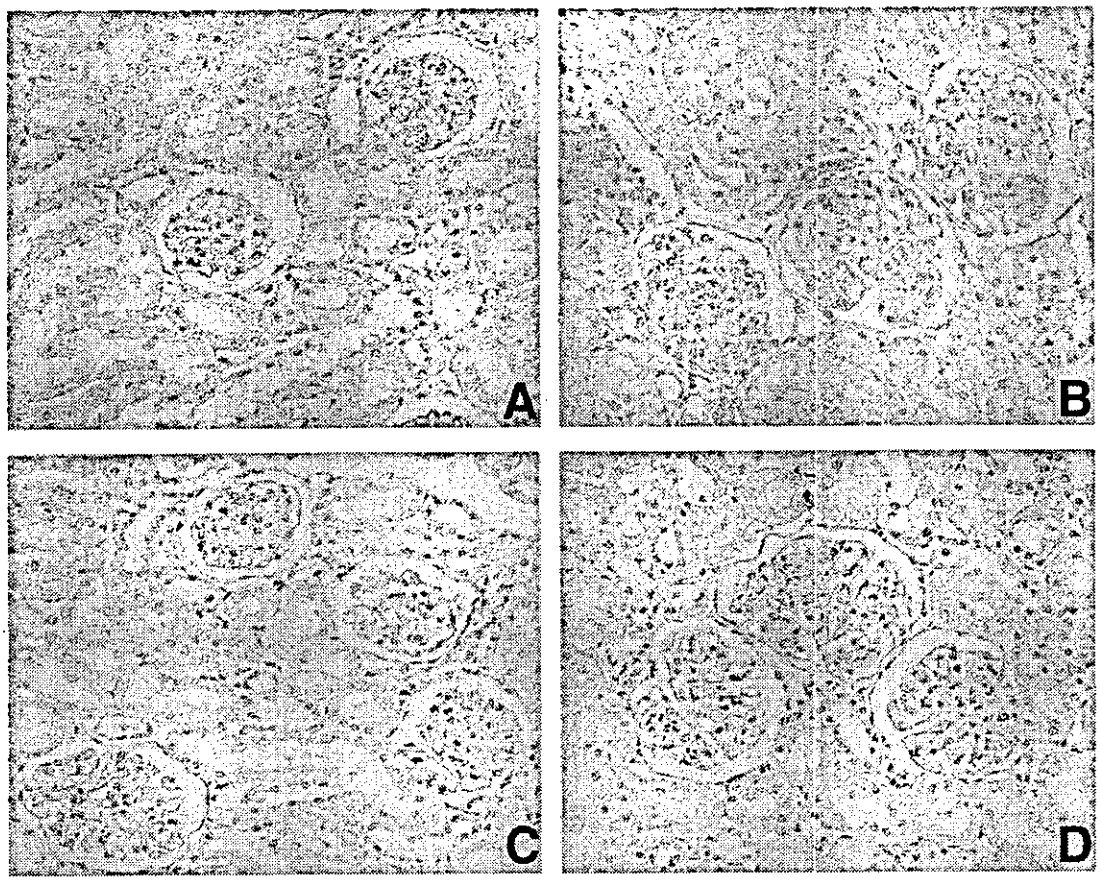

Fig. 3. Morphologic changes induced by anti-Thy-1.1 nephritis can be partially reversed by hemagglutinating virus of Japan (HVJ)/liposome-mediated transfer of specific antisense oligonucleotides (AS ODN) against *Egr-1*. Anti-Thy-1.1 nephritis was induced by injection of monoclonal antibody (mAb) ER4. On day 3 of nephritis, AS2 ODN containing HVJ/liposomes were injected into the left kidney and kidneys were removed on day 6 of nephritis. Hematoxylin & eosin–stained 2 μm sections of kidneys from healthy control rats *(A)*, day 6 nephritic rats *(B)*, and the left *(C)* and right *(D)* kidney of AS2 ODN–injected day 6 nephritic rats are shown (×400).

stantiated by our in vitro observations, where inhibition of *Egr-1* expression by specific AS ODN prevented mitogen-induced mesangial cell proliferation [3]. In these studies, in cultured mesangial cells, we identified specific AS ODN that selectively inhibited *Egr-1* protein expression, whereas the expression of *c-fos* or *c-jun*, two other members of the immediate early gene transcription factor family, was unaffected [3, 4]. Several AS ODNs were used and the inhibitory action of AS ODN on mesangial cell proliferation directly correlated with their ability to inhibit *Egr-1* protein expression. AS ODN that had no effect on *Egr-1* protein did not influence mesangial cell proliferation. Sense, scrambled, and especially mutated (switch of 4 base pairs) control ODN were designed and proved to be without effect on *Egr-1* protein expression or mesangial cell proliferation [3].

The aim of the present study was to establish a causal relationship between *Egr-1* induction and mesangial cell proliferation in vivo. For this purpose we chose the mesangioproliferative anti-Thy-1.1 GN model and transferred specific AS ODN against *Egr-1* into the mesangial compartment on day 3 of the disease by the HVJ/liposome gene transfer method. The HVJ/liposome method was successfully applied in the past to demonstrate the role of PDGF and TGF-β in glomerular disease [42, 47].

The HVJ/liposome method allows a targeted transfer of DNA into glomeruli and selectively into nuclei of mesangial cells, as shown by double immunofluorescence studies staining for the mesangial cell Thy-1.1 surface antigen with the OX7 Ab and using FITC-labeled ODN. In successfully transferred animals, 90% to 95% of glomeruli exhibited a strong nuclear fluorescent staining. Only rats that showed a successful transfer of ODN in biopsy probes were used for further tests (approximately 50% of all investigated animals). On a given glomerular cross-section, an estimated 60% of mesangial cells could be targeted. Since we did not investigate different stages during the mesangial cell cycle, it is not known whether predominantly proliferating or rather quiescent mesangial cells incorporated the transferred ODN. We could

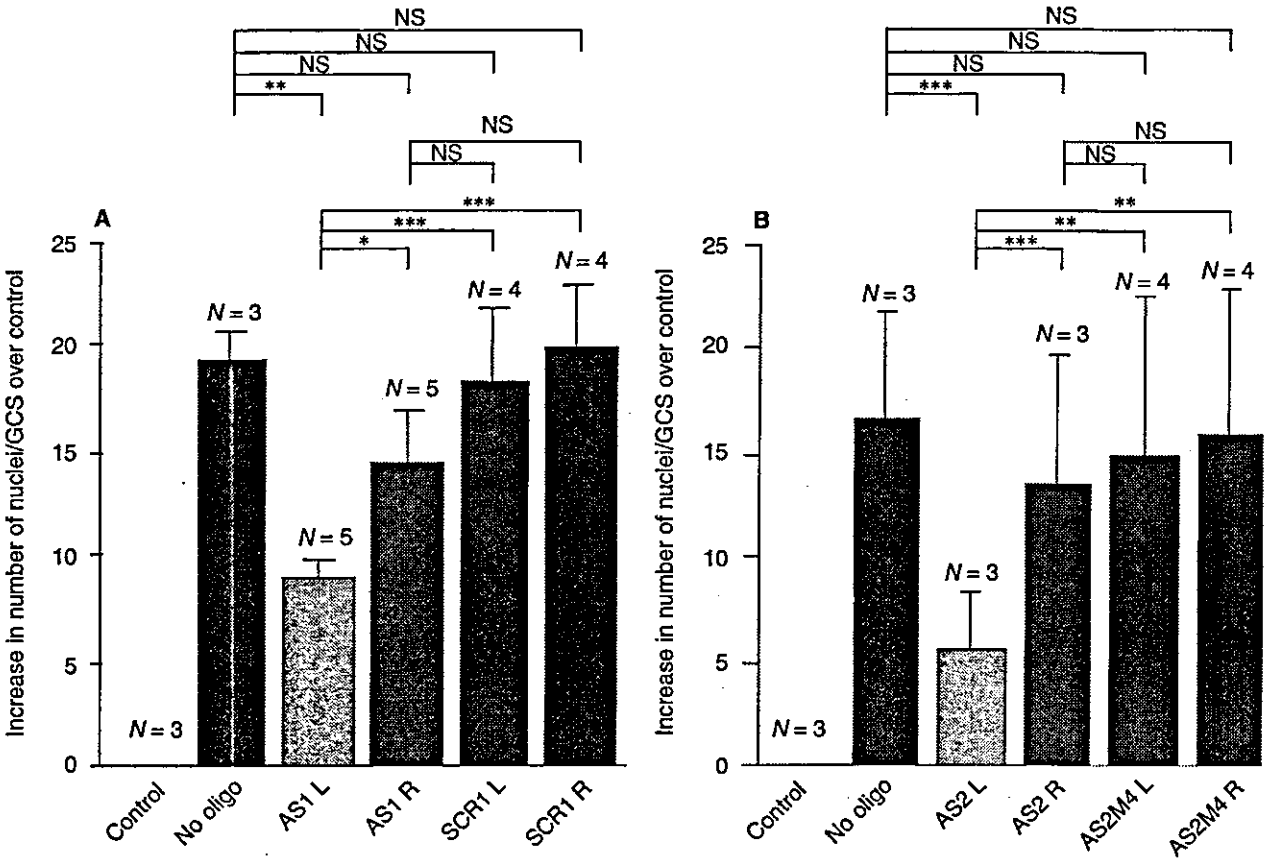

Fig. 4. Transfer of specific antisense oligonucleotides (AS ODN) against *Egr-1* significantly inhibits the increase in glomerular cell number on day 6 of anti-Thy-1.1 nephritis. Three days after induction of anti-Thy-1.1 nephritis AS ODN (AS1 and AS2) or control ODN (SCR1 and AS2M4) containing hemagglutinating virus of Japan (HVJ)/liposomes were injected into the left kidney. On day 6 of nephritis, kidneys were removed and the number of nuclei per glomerular cross-section was evaluated on 2 μm sections of 5% paraformaldehyde (PFA)-fixed paraffin-embedded tissue. Two separate experiments were performed with transfer of ODN AS2 and AS2M4 in *(A)* and AS1 and SCR1 in *(B)*. The increase in the number of nuclei per glomerular cross-section (GCS) over control is shown. The average number of nuclei/GCS in control animals was 47 (A) and 53 (B), respectively. $*P < 0.05$; $**P < 0.01$; $***P < 0.001$.

show, however, that healthy untreated control rats without detectable mesangial cell proliferation could be effectively transferred, demonstrating that resting mesangial cells can be effectively targeted.

In Western blot analyses of glomerular protein we found that *Egr-1* protein expression was reduced by 48% in the left kidney of AS1 ODN–transferred animals. Since not all mesangial cells can be successfully targeted, a higher extent of inhibition was not expected. According to the extent of *Egr-1* protein inhibition, AS ODN against *Egr-1* led to a significant, albeit not complete, inhibition of mesangial cell proliferation. Mesangial cell proliferative activity was determined by counting number of mitotic figures, or of nuclei per glomerular cross-section. In most of our experiments, we observed a minimal, although not significant, inhibitory effect on *Egr-1* induction and mesangial cell proliferation in the right uninjected kidney. We think that this effect is caused by systemic delivery of AS ODN after reperfusion, even though we never detected any fluorescent activity in glomeruli of the right kidney.

The ODN selected for our studies are described in detail in our previous work [3]. The effectivity of ODN depends on sequence-specific target sites within the mRNA; however, no general guidelines for AS ODN selection exist. AS1 and AS2 ODN recognize sequences slightly upstream of the AUG start codon and were the most effective inhibitors of *Egr-1* induction and mesangial cell proliferation in vitro [3, 4] and were therefore used for the in vivo studies. To exclude unspecific effects of ODN, we used two different AS ODNs and various control ODN. The two AS ODN, AS1 and AS2, were capable of inhibiting mesangial cell proliferation and all control ODN were without significant effect. We selected scrambled and mutated control ODN since they have exactly the same relative content of the various nucleotides as the corresponding AS ODN. In the mutated ODN, the T in position 2 was exchanged with the C in

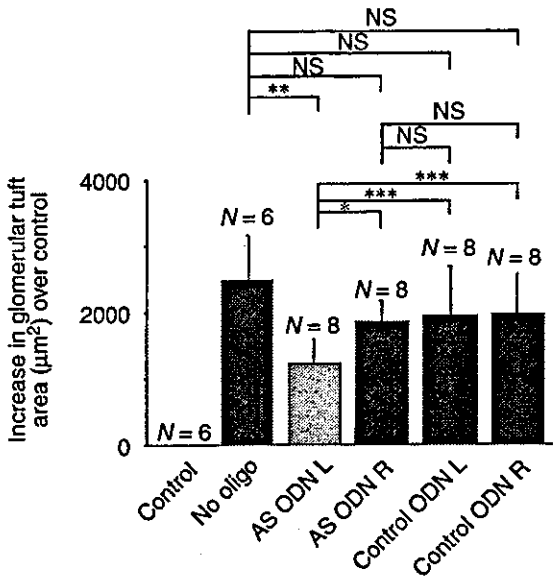

Fig. 5. Transfer of specific antisense oligonucleotides (AS ODN) against *Egr-1* significantly prevents enlargement of glomerular tuft area. Three days after induction of anti-Thy-1.1 nephritis, AS ODN (AS1 and AS2) or control ODN (SCR1 and AS2M4) containing hemagglutinating virus of Japan (HVJ)/liposomes were injected into the left kidney. On day 6 of nephritis, kidneys were removed and tuft area per glomerular cross-section was evaluated on 2 μm sections of 5% paraformaldehyde (PFA)-fixed paraffin-embedded tissue. Increases in glomerular tuft area over control are given. Average glomerular tuft area in control animals was 3896 μm². $^*P < 0.05$; $^{**}P < 0.01$; $^{***}P < 0.001$.

position 8 and the C in position 4 was exchanged with the G in position 14, therefore, even the sequence of nucleotides is maintained in large parts when compared to the corresponding AS ODN. We demonstrated that the AS ODN used were also effective inhibitors of serum-induced *Egr-1* induction and mesangial cell proliferation in cultured rat mesangial cells. Another AS ODN, AS3 was not able to attenuate the increase in *Egr-1* protein after serum stimulation and was also ineffective in blocking mesangial cell proliferation in vitro, further underlining the specific effects of AS1 and AS2 ODN [3].

In addition to the reduction in cell number per glomerular cross-section by transfer of specific AS ODN against *Egr-1* into nephritic kidneys, the enlargement of the glomerular tuft size observed in nephritic animals was significantly reduced in the AS ODN injected left kidney. Glomerular tuft size was not significantly altered in the right kidney of AS ODN–injected animals or in the kidneys of control ODN–injected animals. Since we do not observe any significant differences in *Egr-1* expression, glomerular cell number, number of mitoses, or glomerular tuft size between kidneys of nephritic animals not treated with ODN, and both kidneys of control ODN–treated animals (left kidney injected and subjected to ischemia), we conclude that the HVJ/liposome transfer procedure, including the short ischemia and reperfusion, did not affect glomerular structure.

We did not measure characteristic clinical parameters of glomerular disease activity like proteinuria or hematuria, since only the left kidney was treated with AS ODN against *Egr-1* and the right kidney would still significantly contribute to these markers. It would, however, be very interesting to perform experiments on uninephrectomized nephritic rats in the future and to monitor proteinuria, hematuria, and renal function under these settings.

Our observations, that *Egr-1* is critically linked to the mesangial proliferative response not only in the in vitro but also in the in vivo situation of glomerular inflammation, add to the growing list of recently reported biologic functions of the *Egr-1* protein and further corroborates its role in proliferative processes. Since mesangial cells share many properties of SMC, our data fit very well in line with observations by Santiago et al [36–38], who were able to show that SMC proliferation and regrowth after scraping injury in vitro, but also after balloon injury in the rat carotid artery model in vivo, are critically dependent on the induction of *Egr-1*. With the exception of female infertility, *Egr-1*–deficient mice develop normally, and no apparent phenotype related to disordered growth control becomes evident [27, 28]. Nevertheless, it will be interesting to see how the course of various GN models is altered in *Egr-1*–deficient mice and whether, indeed, a reduced proliferative response can be observed under disease conditions.

The exact role of *Egr-1* in the mitogenic signal transduction cascade is not entirely understood. In its function as a transcriptional activator, *Egr-1* induces the transcription of several target genes some of which, like the PDGF-A chain [17, 18], the PDGF-B chain [34], FGF-2 [20] or cyclin D [25], have been linked to proliferative processes. PDGF-B is strongly up-regulated during experimental mesangioproliferative GN and it was demonstrated by several techniques, including neutralizing antibody infusion [48] or application of aptamers [49], that PDGF exerts a critical role in inducing mesangial cell proliferation. We, therefore, tested whether the *Egr-1* target gene PDGF-B was suppressed in anti-Thy-1.1-nephritis after transfer of AS ODN against Egr-1. A clear down-regulation of PDGF-B protein was observed in nephritic glomeruli transferred with AS ODN against *Egr-1* as compared with nontransferred nephritic glomeruli. We cannot, however, finally prove that reduced PDGF-B expression is a direct consequence of reduced *Egr-1* protein availability or whether reduced PDGF-B expression is due to deactivation and reduced number of mesangial cells, which are the main source of PDGF-B in this model.

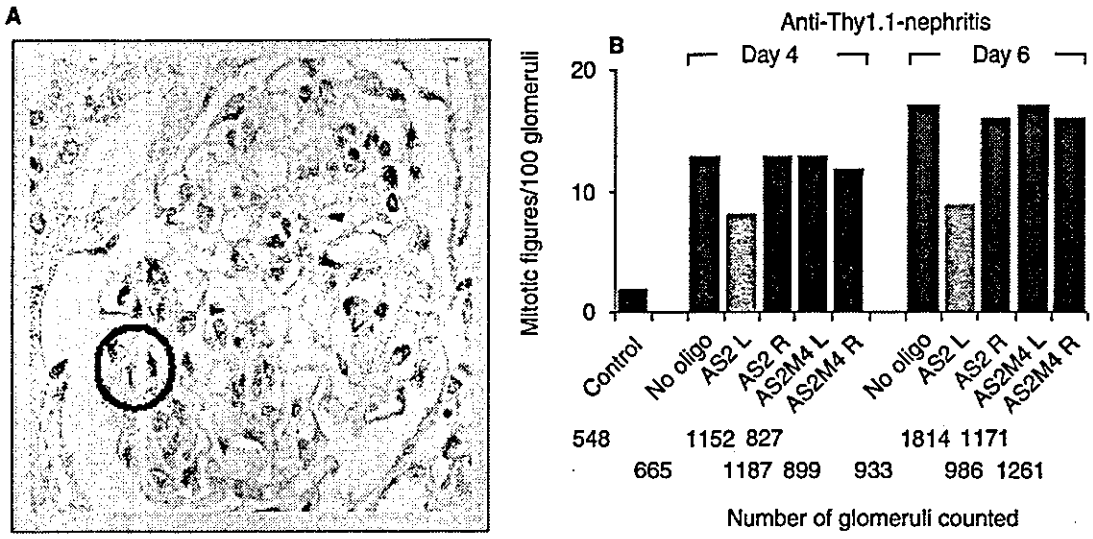

Fig. 6. Transfer of specific antisense oligonucleotides (AS ODN) against *Egr-1* reduces the number of mitotic figures in glomeruli of nephritic rats. Three days after induction of anti-Thy-1.1 nephritis AS ODN (AS2) or mutated control ODN (AS2M4) containing hemagglutinating virus of Japan (HVJ)/liposomes were injected into the left kidney. Kidneys were removed on day 4 and day 6 of nephritis and the number of mitotic figures per 100 glomeruli was counted on 2 μm sections of 5% paraformaldehyde (PFA)-fixed paraffin-embedded kidneys. *(A)* A mitotic figure (anaphase) is shown in a hypercellular area of the glomerular tuft (circled area). *(B)* Number of mitotic figures per 100 glomeruli on day 4 and day 6 of anti-Thy-1.1 nephritis is given. The number of glomeruli counted in three to five animals per experimental condition is indicated.

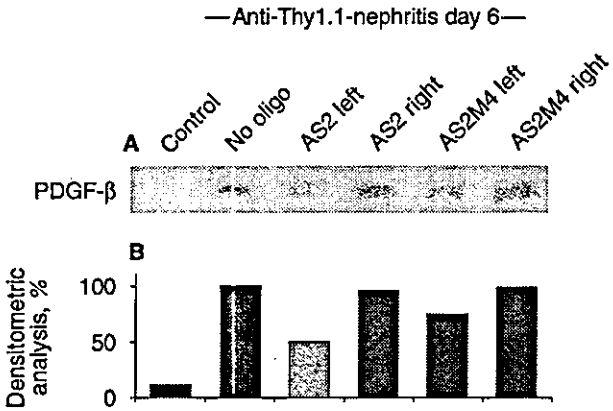

Fig. 7. Inhibition of glomerular platelet-derived growth factor-B (PDGF-B) expression by specific transfer of antisense oligonucleotides (AS ODN) against *Egr-1*. During experimental anti-Thy-1.1 nephritis, ODN were transferred into the left kidney by the hemagglutinating virus of Japan (HVJ)/liposome method. On day 6 of nephritis, kidneys were removed and glomeruli isolated by the differential sieving technique. Glomerular protein lysates (30 μg) from control and day 6 nephritic animals were separated by sodium docedyl sulfate-polyacrylamide gel phoresis (SDS-PAGE) and blotted onto NC membranes. PDGF-B protein was detected by a polyclonal PDGF-B antibody (Ab) using the Pierce Super Signal Detection system. *(A)* Western Blot analysis. *(B)* Densitometric analysis shows glomerular *Egr-1* protein expression in Thy-1.1 animals not treated with ODN is set at 100%.

CONCLUSION

Our data further support the critical role of the transcription factor *Egr-1* in the modulation of cellular growth events. Effective inhibition of *Egr-1* expression by specific AS ODN and consecutive reduction of mesangial cell proliferation can be achieved not only in vitro but also in vivo in experimental mesangioproliferative GN. The identification of additional, potentially kidney-specific target genes of *Egr-1* should add to our understanding of proliferative glomerular processes. Targeting *Egr-1* at the mRNA or protein level or interfering with the expression of its target genes could open new avenues for therapeutic interventions.

ACKNOWLEDGMENTS

The work was supported by a grant by the Deutsche Forschungsgemeinschaft to H.D. Rupprecht (Sonderforschungsbereich 423, TP B1 and Ru 446/3-1). We gratefully acknowledge the technical assistance of Ms. Katja Bruch.

Reprint requests to Prof. Dr. med Harald D. Rupprecht, Med. Klinik - Innenstadt, Ludwig Maximillians University München, Ziemssenstrasse 1, D-80336 München, Germany.
E-mail: Harald.Rupprecht@medinn.med.uni-muenchen.de

REFERENCES

1. Sterzel RB, Rupprecht HD: Response to immune injury: Glomerular mesangial cells, in *Immunologic Renal Diseases,* edited by Neilson EG, Couser WG, Philadelphia, Lippincott-Raven Publishers, 1997, pp 595–626
2. Floege J, Eng E, Young BA, Johnson RJ: Factors involved in the regulation of mesangial cell proliferation in vitro and in vivo. *Kidney Int* (Suppl 39):S47–S54, 1993
3. Hofer G, Grimmer C, Sukhatme VP, *et al*: Transcription factor Egr-1 regulates glomerular mesangial cell proliferation. *J Biol Chem* 271:28306–28310, 1996
4. Rupprecht HD, Hofer G, de Heer E, *et al*: Expression of the transcriptional regulator Egr-1 in experimental glomerulonephritis: Requirement for mesangial cell proliferation. *Kidney Int* 51: 694–702, 1996